

POST-MIDDLE PLIOCENE TECTONIC DEVELOPMENT OF THE NOBLE HILLS,  
SOUTHERN DEATH VALLEY, CALIFORNIA

A thesis submitted to the faculty of  
San Francisco State University  
In partial fulfillment of  
the requirements for  
the Degree

AS  
36  
2016  
GEOL  
• N55

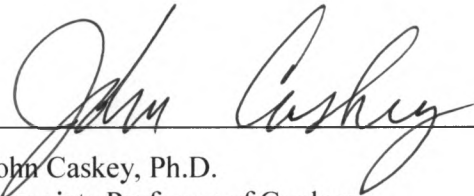
Master of Science  
In  
Geoscience

by  
John Hart Niles  
San Francisco, California  
Fall 2016

Copyright by  
John Hart Niles  
2016

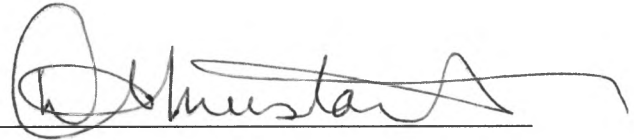
CERTIFICATION OF APPROVAL

I certify that I have read *Post-Middle Pliocene Tectonic Development of the Noble Hills, Southern Death Valley, California* by John Hart Niles, and that in my opinion this work meets the criteria for approving a thesis submitted in partial fulfillment of the requirement for the degree Master of Science in Geoscience at San Francisco State University.



---

John Caskey, Ph.D.  
Associate Professor of Geology



---

David Mustart, Ph. D.  
Professor of Geology



---

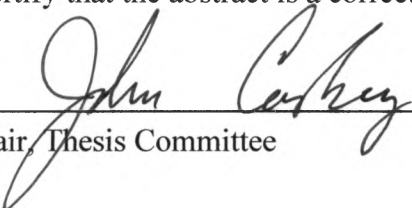
Leonard Sklar, Ph. D.  
Professor of Geology

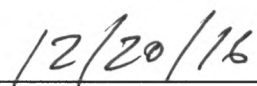
POST-MIDDLE PLIOCENE TECTONIC DEVELOPMENT OF THE NOBLE HILLS,  
SOUTHERN DEATH VALLEY, CALIFORNIA

John Hart Niles  
San Francisco, California  
December 2016

The Noble Hills Formation (NHF) is a ~500 m conformable sequence of generally coarsening-upwards  $\geq 3.34$  Ma basin deposits that is extensively exposed the Noble Hills, southern Death Valley, California. The NHF contains sediments derived from both the Owshead Mountains to the north and Avawatz Mountains to the south. Strata of the NHF display intensive, post-3.34 Ma, northeast-vergent contractional deformation that has previously been interpreted as secondary to contractional deformation along the southern Death Valley fault zone (SDVFZ). Structural and stratigraphic relations and provenance considerations bring into question previous interpretations of large-magnitude, right-lateral offset on the SDVFZ in the Noble Hills. Northeast-vergent contractional deformation in the Noble Hills and greater southern Death Valley is viewed as being driven by clockwise rotation of the northeast Mojave domain about an axis in the Avawatz Mountains, resulting in northeast-directed block movements north of the Garlock fault.

I certify that the abstract is a correct representation of the content of this thesis.

  
\_\_\_\_\_  
Chair, Thesis Committee

  
\_\_\_\_\_  
Date

## ACKNOWLEDGEMENTS

I would like to sincerely thank John Caskey for introducing me to the geology of Death Valley, and for sharing his enthusiasm, insights, and imagination with me on those many long traverses and late nights / early mornings around the campfire in CC Wash. Thanks to those who have helped me in and out of the field: Leslie Bandy, Josh Goodman, John Krueger, Chris Davidson, Jim Calzia, Michelle Haskins, and Brian Melton. Special thanks to my parents, Mardi and Phil Niles for their encouragement and support through this project and beyond.

This work was funded in part by the USGS EDMAP Award No. G11AC20182. The Pestrong Geoscience Research Grant and the Community Foundation's Desert Legacy Fund also provided support for fieldwork.

This study has been greatly aided by the work of Elmira Wan, David Wahl, and Holly Olsen at the USGS tephrochronology lab in Menlo Park.

*"It's too late to worry about the sleep you didn't get last night, and it's too early to worry about the sleep you won't get tonight."*

– J. Caskey and J. Niles, 2010

## TABLE OF CONTENTS

LIST OF TABLES .....	ix
LIST OF FIGURES .....	x
1.0 INTRODUCTION .....	1
2.0 PREVIOUS WORK.....	7
3.0 METHODS .....	15
3.1 Field Mapping and Map Compilation .....	15
3.2 Clast Counts .....	17
3.3 Tephrochronology .....	18
4.0 STRATIGRAPHY .....	20
4.1 Noble Hills Formation.....	21
4.1.1 nh1a – Lower Sandstone and Siltstone Member of the Noble Hills Formation.....	23
4.1.2 nh1b – Gypsiferous Member of the Noble Hills Formation.....	25
4.1.3 nh1c – Halitic Mudstone Member of the Noble Hills Formation.....	28
4.1.4 nh2c and nh2ca – Conglomerate Member of the NHF .....	33
4.1.5 nh2f – Upper Sandstone, Siltstone and Gypsiferous Member of the NHF.	36
4.1.6 nh2mb – Megabreccia Member of the NHF .....	37

4.1.7	nh3 – Granite Bearing Conglomerate of the NHF .....	40
4.2	Tertiary Fanglomerates .....	43
4.3	Quaternary Alluvium.....	44
4.3.1	Qoa – Middle-Early Pleistocene Alluvial Fan Deposits .....	44
4.3.2	Qa2 – Middle Pleistocene Alluvial Fan Deposits .....	45
4.3.3	Qa1 – Late Pleistocene Alluvial Fan Deposits .....	45
4.3.4	Qya3 – Middle Holocene Alluvial Fan Deposits.....	45
4.3.5	Qya2 – Late Holocene Alluvial Fan Deposits .....	46
4.3.6	Qya1 – Late Holocene Alluvial Fan Deposits .....	46
5.0	STRUCTURAL GEOLOGY .....	48
5.1	Northeast Vergent Contractional Structures in the Noble Hills.....	49
5.2	North-Striking Right Lateral Faults .....	56
5.3	Southern Death Valley Fault Zone in the Vicinity of the Noble Hills.....	57
5.3.1	Surface Traces of the SDVFZ in the Noble Hills .....	57
5.3.2	Constraints on post-middle Pliocene Offset along the SDVFZ.....	65
5.3.3	Constraints on longer-term offsets on the SDVFZ .....	68
6.0	SUMMARY AND DISCUSSION.....	73
6.1	Summary and Interpretation of the Noble Hills Formation .....	73
6.2	Transrotation of the Northeast Mojave Block and Tectonic Development of Southern Death Valley .....	75

7.0 CONCLUSIONS.....	82
REFERENCES .....	83
APPENDICES .....	88

## LIST OF TABLES

Table	Page
1. Slip rate estimates for the NDVFZ and SDVFZ.....	3
2. Summary of alluvial fan surface characteristics and nomenclature.....	16

## LIST OF FIGURES

	Page
Figure 1: Map of the eastern California shear zone (ECSZ) showing major faults and structural domains .....	5
Figure 2: Simplified map of the Death Valley fault system. ....	6
Figure 3: Tectonic and geographic setting of the Noble Hills and the southern Death Valley fault zone .....	13
Figure 4: Generalized geologic map of the northern Avawatz Mountains and Noble Hills from Brady .....	14
Figure 5: Illustration of progressive development of surface morphology for alluvial fan units.....	17
Figure 6: Index map of the Noble Hills .....	19
Figure 7: Correlation of units of the Noble Hills Formation. ....	23
Figure 8: Sedimentologic characteristics of the lower sandstone and siltstone member of the Noble Hills Formation .....	27
Figure 9: Highly sheared mylonitic gypsum within nh1b member .....	28
Figure 10: Massive, crystalline halite .....	30
Figure 11: Contact between nh1c and nh2c in the Niter Field area.....	31
Figure 12: Representative contacts between members of the NHF. ....	32
Figure 13: Avawatz-sourced conglomerate member (nh2ca) exposed in the Canadian Club Wash area .....	35
Figure 14: Mixed lithology conglomerate (nh2c) exposed in the Niter Field area.....	36

Figure 15: View of Niter Field area showing contact between the granite bearing conglomerate (nh3) and older sandstone of nh2f.....	41
Figure 16: Granite bearing conglomerate .....	42
Figure 17: Contact between capping conglomerate Tf3 and upper sandstones and siltstones (nh2f).....	44
Figure 18: Histogram plots of clast composition percentages for conglomeratic units in the Noble Hills Formation .....	47
Figure 19: Cross section B-B' of the CC Wash area.....	53
Figure 20: Generalized fault map of the southern Noble Hills.....	54
Figure 21: Exposure of CC thrust in the Canadian Club Wash area .....	55
Figure 22. Axial Ridge fault between Canadian Club and Amphitheater washes.....	56
Figure 23: SDVFZ trace61	
Figure 24: Trace of the SDVFZ in the CC Wash area.....	62
Figure 25: Cross section A-A' though the Niter Field area .....	63
Figure 26: High-angle fault in the Niter Field area of the northern Noble Hills .....	64
Figure 27: Geologic map of the Canadian Club Wash area.....	66
Figure 28: Map of the northeast Avawatz Mountains and Southern Salt Spring Hills.....	71
Figure 29: Oblique view of the Avawatz Mountains and Southern Salt Spring Hills.....	72
Figure 30: Model of progressive deformation of the Noble Hills and Confidence hills basin deposits as the result of clockwise rotation of the Mojave Block. ....	79
Figure 31: Cartoon block model illustrating rotational model of the northeast Mojave domain modified from Schermer et al. (1996).80	
Figure 32: Model of mechanism for north-striking faulting in the Noble Hills .....	81

## LIST OF APPENDICES

Appendix	Page
I. Clast count data .....	89
II. Tephrochronology lab results.....	90

## 1.0 INTRODUCTION

The Noble Hills are located in the southernmost part of the Death Valley region, in southeast California (Figure 1 & 2). They extend northwest from the foothills of the Avawatz Mountains for a distance of 17 km. The Noble Hills trend parallel to, and form the principal physiographic feature aligned with strands of the of the right-lateral southern Death Valley fault zone (SDVFZ) as depicted on published maps (Figures 1 & 3) (Jennings et al., 1963). The SDVFZ makes up the southern component of the Death Valley fault system (DVFS) (Machette, 2001), which also includes the northern Death Valley fault zone (NDVFZ), Fish Lake Valley fault zone (FLVFZ), and the Black Mountains fault zone (BMFZ) in central Death Valley (Figure 1). Right-lateral shear along the DVFS accounts for a significant part of the regional shear associated with the Eastern California shear zone (ECSZ) (Dokka and Travis, 1990) (Figure 1). Distributed right-lateral shear across the ECSZ accommodates up to 25% (12 mm/yr) of the overall relative motion between the Pacific and North American plates (Miller et al., 2001). The ECSZ in southeast California lies well east of the San Andreas fault system, and is generally considered to mark the diffuse boundary between the Sierra Nevada microplate and the North American plate (e.g., Unruh et al., 2003).

The SDVFZ together with the NDFVZ have been described by Burchfiel and Stewart (1966) as forming a ~35 km right-step-over (Figure 2), across which right-lateral offset is transferred. Slip transfer across the ‘releasing’ step-over geometry has resulted in

a central Death Valley pull-apart basin, which is formed by normal-right-oblique slip along the BMFZ and faults on the west side of Death Valley (Figures 1 & 2). Requisite to this Burchfiel and Stewart (1966) pull-apart model is that the slip histories along the NDVFZ and SDVFZ have been similar during the time of development of the pull-apart basin. However, studies bearing on long-term slip rates of these faults systems suggest that magnitude and timing of offsets along the SDVFZ are much lower than those determined for the NDVFZ (Table 1).

Slip estimates for the NDVFZ range from 8 km (Klinger and Sarna-Wojcicki, 2001) since the Pliocene, and 4 km since the (middle?) Pleistocene (Klinger, 1999). Slip rates calculated from these offsets show that a significant amount of the slip budget for the ECSZ north of the Garlock fault zone is accommodated by the NDVFZ (Klinger, 1999; Klinger, 2001; Klinger and Sarna-Wojcicki, 2001; Klinger, 2002, Frankel et al. 2007a; Frankel et al., 2007b) (Table 1).

Estimates of post-early-late Miocene and Quaternary right-lateral displacements on the SDVFZ range from 20-35 km to 8 km, respectively (Brady, 1984, 1999; Butler, 1988). Conversely, Green (2009) and Goodman (2010) determined offsets of 420 m and 600 m, respectively, along the only mappable (e.g., visible) strands of the SDVFZ observed in the northern half of southern Death Valley (SDV). Cross cutting relationships the Confidence Hills require that the initiation of movement along the fault zone is less than 1.1-0.9 Ma.

<b>Fault Name</b>	<b>Slip Rate (mm/yr)</b>	<b>Time Period</b>	<b>Reference</b>
<b>SDVFZ</b>	~0.31	post-late Pleistocene	Wright and Troxel, 1984
	~0.7	post-late Pleistocene	Goodman, 2010
	0.2	post-late Pleistocene	Green, 2009
<b>NDVFZ</b>	2.5 - 3	post-late Pleistocene	Frankel et al., 2007b
	4.2 - 4.7	post-late Pleistocene	Frankel et al. 2007a
	4 - 9	post-late Pleistocene	Klinger, 2001
	2 - 3	post-late Pliocene	Klinger and Sarna-Wojcicki, 2001
	3 - 6	Holocene	Klinger, 2002
	3 - 5	post-late Pleistocene	Klinger, 1999

Table 1: Slip rate estimates for the NDVFZ and SDVFZ

Previous workers recognized the significant contractional deformation in the Noble Hills and the Confidence Hills and interpreted this deformation as coincident with and directly related to major distributed right-lateral shearing along the SDVFZ (Noble and Wright, 1954; Stamm, 1981; Brady, 1984, 1986a; Butler et al., 1984; Dooley and McClay, 1996). In contrast, locally intensive northeast-vergent shortening documented in the Confidence Hills (Goodman, 2010) was found to predate the initiation of the SDVFZ rather than to have formed as secondary deformation along the SDVFZ as interpreted in earlier studies.

This report presents a significantly improved understanding of the tectonic history of the Noble Hills largely based on major revisions to the stratigraphic framework and new tephrochronology for middle-to-late Pliocene deposits extensively exposed along the northeast side of the Noble Hills, which are herein referred to informally as the Noble

Hills Formation (NHF). Map relations together with provenance determinations for Pliocene conglomerates and megabreccia deposits of the NHF are used to place limiting constraints on right-lateral offsets along the SDVFZ. Similar to recent findings in the Confidence Hills, major folding and thrusting in the eastern Noble Hills is strongly northeast-vergent, without exception, and the major episode of northeast-directed contraction appears to predate the initiation of movement on any identifiable strands of the SDVFZ in the Noble Hills area. The large-magnitude right-lateral offsets interpreted by earlier workers are not supported by relations along mapped faults or considerations of provenance for conglomerate and megabreccia units that make up a large part of the NHF. The kinematics of Pliocene-to-recent deformation in the Noble Hills are discussed in the context of transrotation and northward impingement of the northeast Mojave Block in the southern Death Valley region (Garfunkel, 1974; Carter et al., 1987; Schermer et al., 1996; Schermer et al., 1996), and the evolution of the ECSZ in the region.

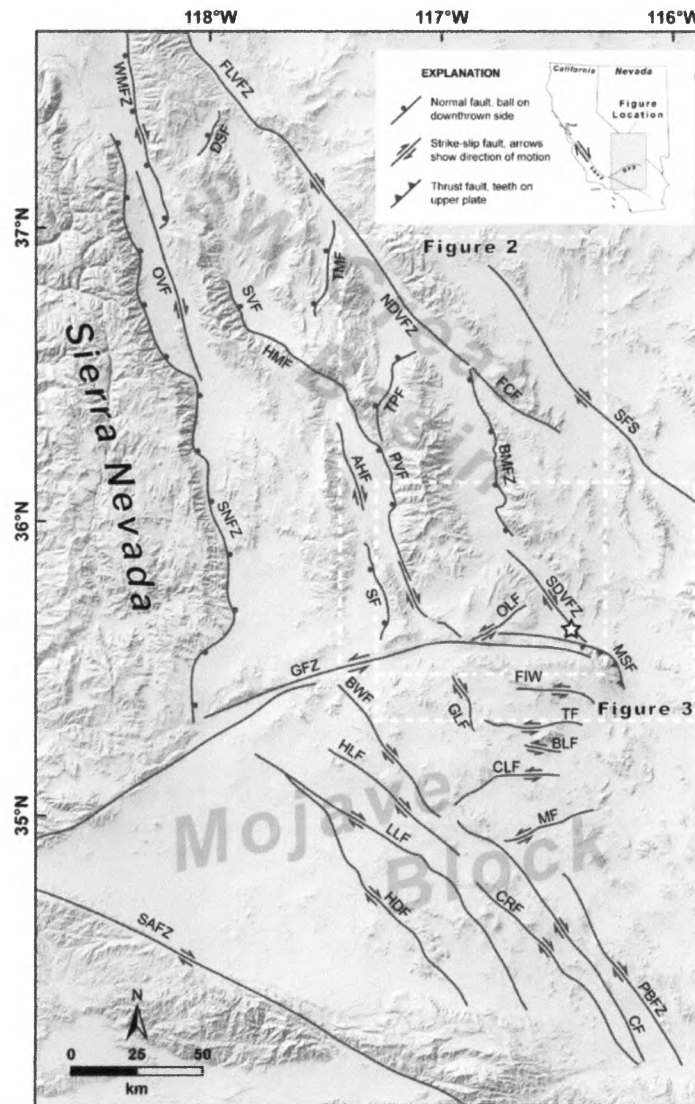


Figure 1: Map of the eastern California shear zone (ECSZ) showing major faults and structural domains. Dashed white outlines show areas of Figs. 2 and 3. White star shows study area of the Noble Hills. AHF—Ash Hill fault, BLF—Bicycle Lake fault, BMFZ—Blackwater fault, BWF—Blackwater fault, CF—Calico fault, CLF—Coyote Lake fault, CRF—Camprock fault, DSF—Deep Springs fault, FCF—Furnace Creek fault, FIF—Fort Irwin fault, FLVFZ—Fish Lake Valley fault zone, GFZ—Garlock fault zone, GLF—Goldstone Lake fault, HDF—Helendale fault, HLF—Harper Lake fault, HMF—Hunter Mountain fault, LLF—Lockheart-Lenwood fault, MF—Manix fault, MSF—Mule Springs fault, NDVFZ—Northern Death Valley fault zone, OLF—Owl Lake fault, OVF—Owens Valley fault, PBF—Pisgah-Bullion fault zone, PVF—Panamint Valley Fault, SAFZ—San Andreas fault zone, SDVFZ—Southern Death Valley fault zone, SF—Searless Valley fault, SFS—Stateline fault system, SNFZ—Sierra Nevada fault zone, SVF—Saline Valley fault, TF—Tiefort Mountain fault, TMF—Tin Mountain fault, TPF—Towne Pass fault, WMFZ—White Mountains fault zone. Fault locations adapted from Jennings (1994).

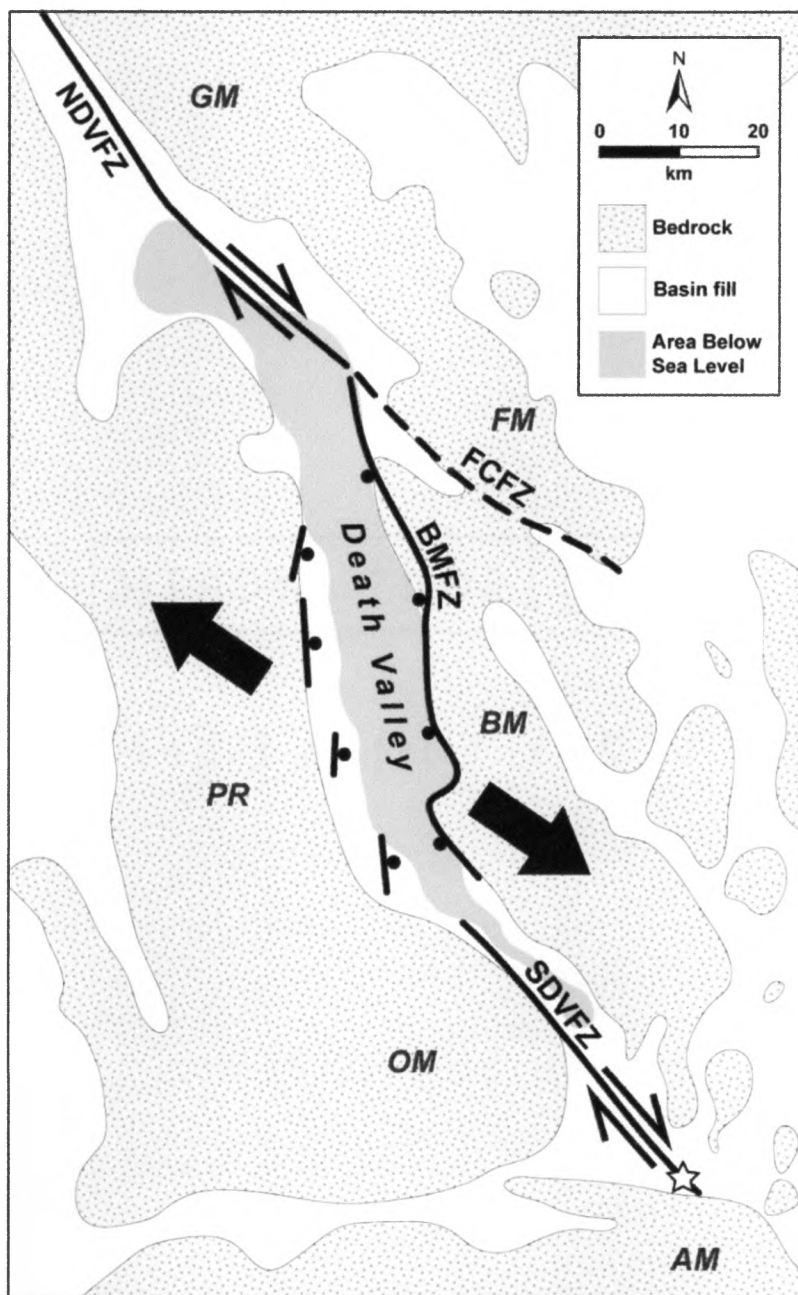


Figure 2: Simplified map of the Death Valley fault system. The conventional interpretation for central Death Valley is that it is a pull-apart basin (Burchfiel and Stewart, 1966) formed at the ~35 km releasing step-over between the right-lateral northern Death Valley and southern Death Valley fault zones (NDVFZ and SDVFZ). White star shows approximate location of the Noble Hills study area. AM—Avawatz Mountains, BMFZ—Black Mountains fault zone, FCFZ—Furnace Creek fault zone (pre-Quaternary), FM—Funeral Mountains, GM—Grapevine Mountains, OM—Owlshead Mountains, PR—Panamint Range.

## 2.0 PREVIOUS WORK

Early reconnaissance and geologic mapping within the Noble Hills conducted by Noble and Mansfield (1922), Ver Planck (1952), and Durrell (1953) focused primarily on mineral deposits of economic potential that are commonly contained in the basin deposits of the Noble Hills strata (e.g., salt, celestite, and gypsum). Johnson and Lewis (1952) first interpreted several of the abrupt, subvertical lithologic boundaries in the Noble Hills as northwest-striking faults.

The initial studies bearing on the question of large-magnitude dextral offsets in the Death Valley region were motivated by the regional oroclinal patterns, and inferred clockwise rotation and right-lateral offsets of isopach trends in Precambrian and Paleozoic strata (Stewart, 1967; Hamilton and Meyers, 1966; Wright and Troxel, 1967). High-end estimates of right-lateral displacements vary from 80 km (Stewart, 1967) to 50 km (Hamilton and Meyers, 1966). Using the same isopach data, Wright and Troxel (1967) alternatively proposed that right-lateral displacement across the SDV region could be as little as 8 km. Subsequent estimates of right-lateral offset more specific to strands of the SDVFZ as depicted on earlier maps of the region were necessarily based on the details of the geology mapped and interpreted along the fault within the mountain ranges in greater southern Death Valley region.

Troxel and Butler (1979) provided the first somewhat detailed geologic map of the Noble Hills, which characterized the SDVFZ as a zone of multiple, subparallel, overlapping right-lateral fault strands extending the length of the Noble Hills and

terminating to the south along the northeast flank of the Avawatz Mountains (Figure 3). Map units were distinguished primarily on the basis of lithologic characteristics. Numerical dates were not yet available for the well-exposed basin deposits of the Noble Hills, and so stratigraphic ages were only estimated from crude correlations to lithologically similar strata of known ages elsewhere in the region. Troxel and Butler (1979) suggested that cumulative right-lateral offset along the SDVFZ was likely on the order of “sever miles”, though the timing of offset was not estimated. Additionally, Troxel and Butler (1979) interpreted the SDVFZ as terminating along the northeastern flank of the Avawatz Mountains.

Perhaps the most commonly cited work regarding estimates of large-magnitude right-lateral displacement on displacement on the SDVFZ is from a subsequent study by Butler et al. (1988) who interpreted ~35 km of post-mid-Miocene right-lateral displacement along a cryptic strand of the fault zone (i.e., “western subzone”) (Figure 4, offset marker 3). The estimated offset was based on the restoration of alluvial gravels observed along the eastern range front the Owshead Mountains to their presumed source area along southern Panamint Range (Figure 3, offset marker 2). Map relations therefore required that their “western subzone” must lie concealed at the eastern base of the Owshead Mountains range front. Since the time of Butler et al.’s (1988) report the evidence for large-magnitude offset and an inferred strike-slip fault at the Owshead Mountains range front has been found to be erroneous based on a later discovery by the same authors (unpublished) of alluvial gravels within the Owshead Mountains (i.e., west of the

inferred western subzone fault) with the same source area as those found along the range front (B. Troxel, personal communication to J. Caskey, SFSU, 2009). This later observation negates the need for cryptic 'western subzone' fault (Butler et al., 1988) and further suggests that these gravels were more likely transported to their present location by fluvial rather than tectonic processes.

Brady (1984, 1986a) conducted geologic mapping for the northern Avawatz Mountains and new field studies of the Noble Hills region building on earlier studies of Troxel and Butler (1979). Brady (1984, 1986a) proposed a stratigraphic framework for the Noble Hills, dividing the area into an older central and a younger eastern belt based on differences in overall lithologic makeup and inferred relative age, and further subdivided these belts into informal mappable units. Of particular note, Brady (1984, 1986a, Brady and Troxel, 1999) proposed large-magnitude dextral offset along the SDVFZ in the Noble Hills based on assumed source area in the Halloran Hills for distinctive clasts of ptlygmatically folded Proterozoic gneiss and Mesozoic(?) granite found within the early-Late(?) Miocene Military Canyon Formation which Brady and Troxel (1999) formally named for exposures between the southernmost part of the Noble Hills and the Avawatz Mountains (offset marker 1, Figure 3). Based on east-to-west paleocurrent data from the Military Canyon Formation, Brady interpreted 20-23 km of right-lateral offset along an inferred southward continuation of the SDVFZ that would allow the Halloran Hills to be restored to a location east of the Noble Hills. Brady and Troxel (1999) assigned an early-Late Miocene age for the Military Canyon Formation

based on a speculative correlation of tephra layers found in both the Military Canyon Formation and the 11.0 Ma Avawatz Formation (K-Ar; sanidine; Brady and Troxel, 1999), which reportedly share similar shard morphologies and major trace element chemistry. Therefore, the large right-lateral displacement interpreted between the Halloran Hills and the northern piedmont area of the Avawatz Mountains is considered by Brady (1984, 1986a) to be post-early-Late Miocene.

Brady (1986a, 1986b) also proposed a minimum of 8 km of right-lateral offset along strands of the SDVFZ lying within the Noble Hills based on the inferred displacement of Owlshead-Mountain-derived fanglomerate found in the eastern Noble Hills from a postulated location that would be more proximal to the Owlshead Mountains (offset marker 1, Figure 3). Brady's (1986a, 1986b) interpreted offset and assumption of Quaternary age for these Owlshead Mountain-derived fanglomerates suggested a slip rate of about 3 mm/yr. Troxel (1994) proposed a right-lateral offset of approximately 28 km along a single strand of the SDVFZ based on the presence of gneissic and volcanic clasts within the Owlshead-Mountain-derived fanglomerate in the northern Noble Hills, which were interpreted to have been derived from the northeast Owlshead Mountains. Timing of displacement along this strand was interpreted by Troxel (1994) to be younger than 14 Ma and older than the Pleistocene Confidence Hills strata.

This study presents new tephrochronology data that establishes a late Pliocene (~3.34 Ma) age for the Owlshead Mountain-derived fanglomerate. Additionally, this study presents a significantly revised stratigraphic framework for sedimentary units on

the eastern side of the Noble Hills (i.e., the Noble Hills Formation) and reevaluates the evidence cited by Brady (1986a, 1986b) and Troxel (1994) for large right-lateral offsets along the SDVFZ based on structural and stratigraphic relations in the Noble Hills and provenance considerations for conglomerate and megabreccia units of the Noble Hills as a whole.

The Pleistocene slip history of the SDVFZ has recently been investigated by Goodman (2010) along the Confidence Hills section of the SDVFZ and Green (2009) along the northern part of the Noble Hills section.

Goodman (2010) documented intensive northeast-vergent fault propagation folding (inferred blind thrusting) involving a conformable section of the Confidence Hills Formation dated at 2.3-1.0 Ma. Clear cross cutting relations in the Confidence Hills show that northeast-vergent folding predates initiation of the SDVFZ in that area, and that net post-1.0 Ma offset along the only mappable trace of the SDVFZ is tightly constrained to be only 600 m where it cuts obliquely across previously folded strata. The timing of initial movement along the fault is constrained only to be after ~1.0 Ma, yielding an average slip-rate of 0.6 m/ka. This average slip-rate is considered a minimum rate because the age of initiation of strike-slip faulting is only constrained to be post~1.0 Ma.

Similarly, Green (2009) examined highly folded late Pliocene strata across a restraining step-over at the north end of the Noble Hills section of the SDVFZ. Green estimated a net offset of approximately 420 m using net shortening of the folded strata which contain the ~3.34 Ma Mesquite Springs tephra as a proxy for slip transfer across a

persistent restraining step-over on the SDVFZ. The 420 m of shortening is considered a minimum for the inferred amount of slip transfer for a number of cited reasons and so the net post-3.34 Ma offset in this area is remarkably similar to the post-1.0 Ma offset of 600 m determined in the Confidence Hills, suggesting similar slip histories for the two areas. The 420 m of post-3.34 Ma right-lateral offset estimated for the SDVFZ by Green is more than an order of magnitude lower than the 6-8 km offset estimated for the NDVFZ over the same time frame.

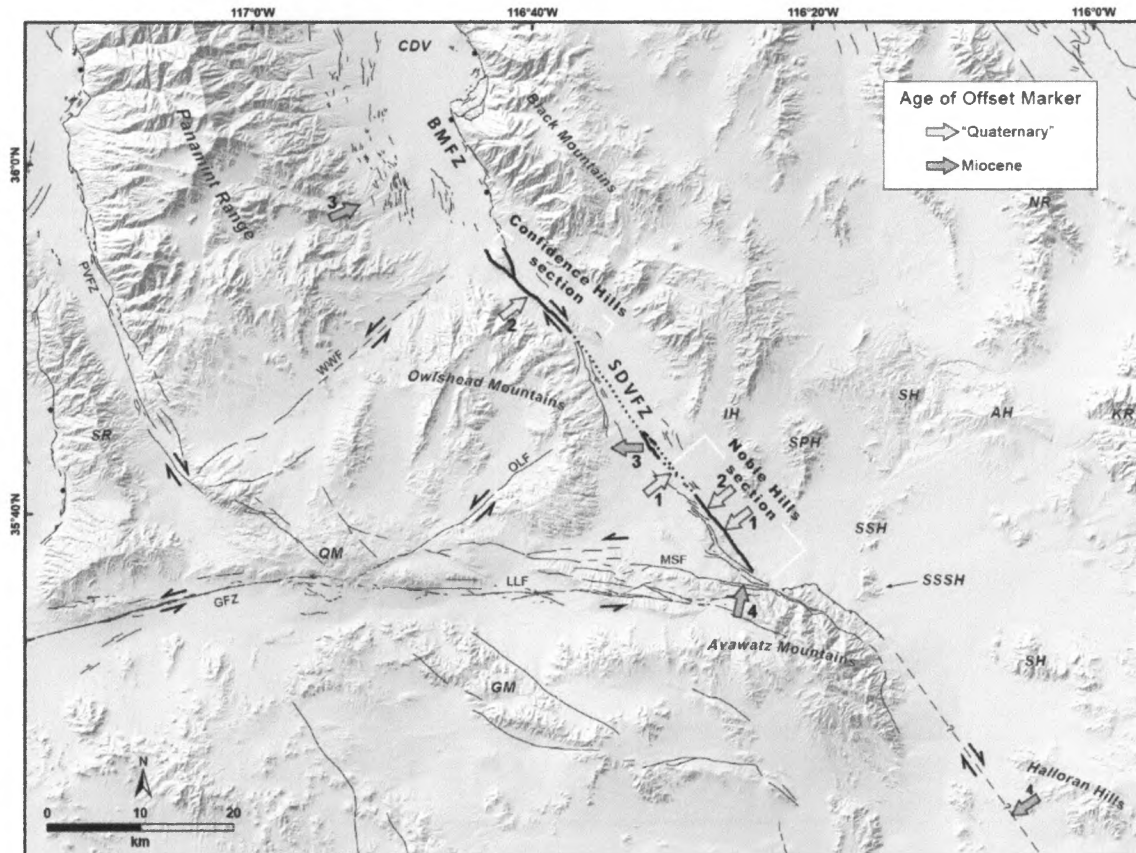


Figure 3: Tectonic and geographic setting of the Noble Hills and the southern Death Valley fault zone (SDVFZ). Active traces of the SDVFZ are shown in bold, dotted where concealed. Colored arrows mark the locations of features used by previous workers to estimate right-lateral offset along the SDVFZ; numbers on arrows refer to 1) Brady, 1986a, 1986b, 2) Troxel, 1994, 3) Butler et al. 1988, and 4) Brady and Troxel, 1999. Abbreviations for faults used: BMFZ – Black Mountains fault zone, GFZ—Garlock Fault Zone, LLF—Leach Lake fault, MSF—Mule Springs fault, OLF—Owl Lake Fault, PMFV – Panamint Valley fault zone, SDVFZ—southern Death Valley fault zone, WWF – Wingate Wash fault. Abbreviations for geographic features used: AH—Alexander Hills, CDV – Central Death Valley, GM—Granite Mountains, IH—Ibex Hills, KR—Kingston Range, NP—Nopah Range, QM—Quail Mountains, SH—Sperry Hills, SPH—Saddle Peak Hills, SR—Slate Range, SSH—Salt Spring Hills. Faults are from Jennings (1994); approximate location of the Wingate Wash fault location from Luckow et al. (2005); southern continuation of the SDVFZ south of the Avawatz Mountains approximated from Brady (1984, 1999).

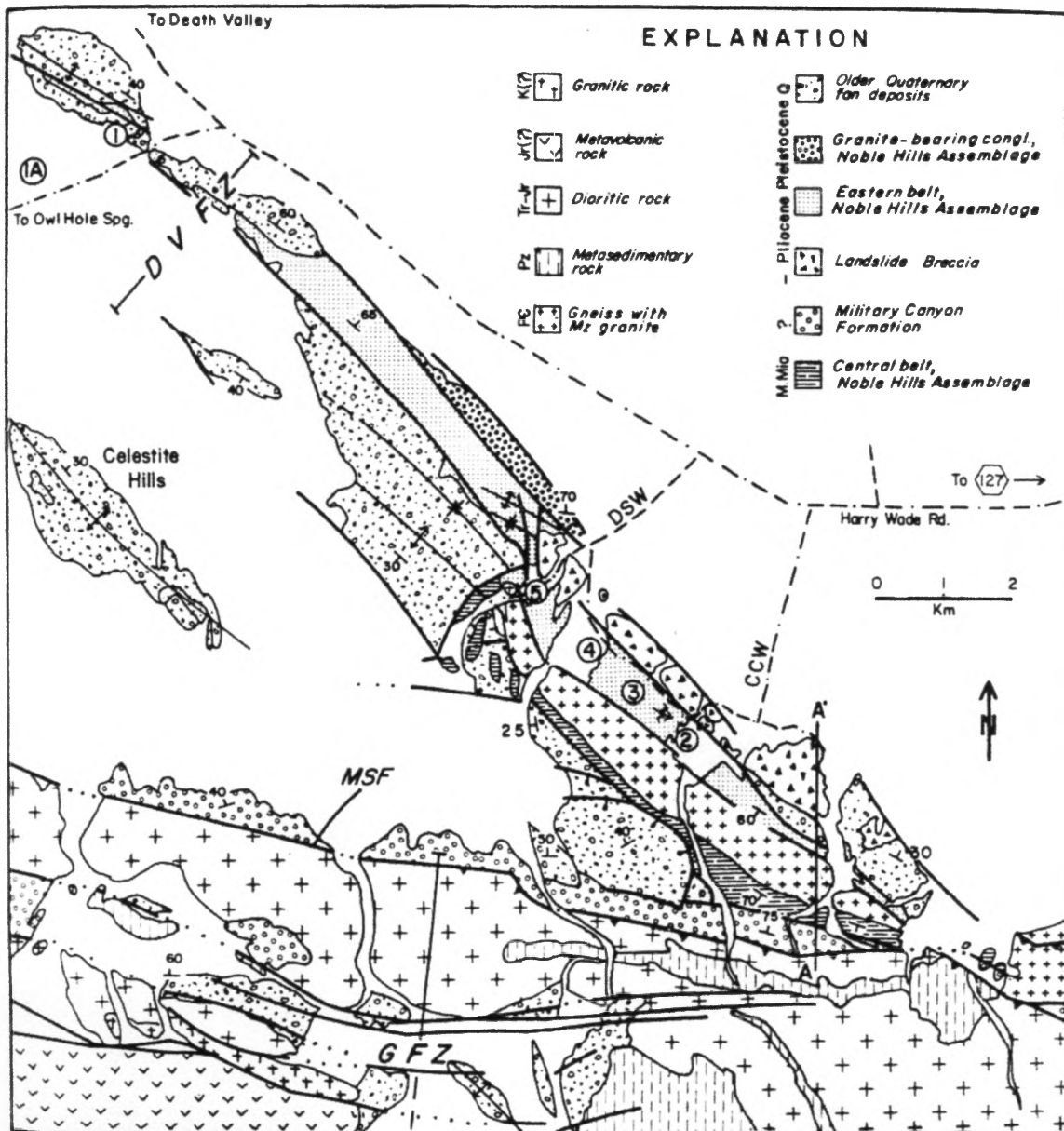


Figure 4: Generalized geologic map of the northern Avawatz Mountains and Noble Hills from Brady (1986b) showing locations of mapped strands of the SDVFZ and the “granite-bearing conglomerate”. DVFZ – Death Valley fault zone (reassigned as the SDVFZ by Machette, 2001), GFZ – Garlock fault zone, MSF – Mule Spring Fault, CCW – Canadian Club Wash, DSW – Denning Spring Wash.

### **3.0 METHODS**

#### **3.1 Field Mapping and Map Compilation**

Mapping of the Noble Hills study area was conducted in the field using orthorectified, high-resolution, full color, digital satellite imagery produced by the United States Department of Agriculture's National Agriculture Imagery Program (NAIP). The scale of the NAIP imagery base maps varied depending on the resolution required for a given area, although 1:6,000-scale base maps were mostly used in the field.

An area of approximately 40 km<sup>2</sup> was mapped in detail. Numerous reconnaissance traverses in the region were required to field-check previous work and to better understand the history of the Noble Hills in the context of regional geologic relations. Sedimentological specifically clast counts from various conglomeratic units of the Noble Hills Formation were collected for the purpose of understanding provenance, and aspects of depositional environments. Structural data was collected to construct cross sections through three areas within the Noble Hills that display representative deformation (Plate 1), namely Canadian Club Wash (CCW), Salt Basin (SB), and the northern Niter Field (NF) areas. All field data were compiled in ArcGIS 10.1 software to produce a geologic map of the Noble Hills at a scale of 1:12,000 (Plate 1). Areas to the southwest and northeast of the Noble Hills were compiled from the work of Brady (1986a) and Green (2009), respectively, and these areas are delineated on the Plate 1 inset.

To facilitate construction of the cross section in the CCW area (Plate 1), numerous digital photographs of vertical exposures taken consecutively along a traverse

approximately perpendicular to bedding and structures were stitched together in Adobe Photoshop to create a seamless panoramic image. The cross section was drafted in the field using the panoramic image as a base.

Detailed field mapping of alluvial fan deposits units was not within the scope of this study; however, fan units were mapped in reconnaissance using NAIP imagery and a modified version of the chronostratigraphic framework developed for surficial deposits in the Mojave Desert region by Miller and Menges (2007) (Table 1). Map unit designations and relative ages for alluvial units were primarily based on inset relations and surface characteristics that could be observed on NAIP imagery.

Miller and Menges (2007) Map Units	This Study	Age	Surface Topography	Desert Pavement	Desert Varnish	Age
Qya1	Qya1	Holocene	active fans	none	none	<15 ka
Qya2	Qya2	Holocene	strong bar & swale	none	none to very weak	<15 ka
Qya3	Qya3	Holocene	remnant bar & swale	incipient	weak	<15 ka
Qya4		early Holocene	weak remnant bar & swale	weak	weak to moderate	<15 ka
Qia1	Qa1	late Pleistocene	flat, faint bar & swale	weak to moderate	moderate	30-250 ka
Qia2	Qa2	late Pleistocene	flat	moderate to strong	moderate to strong	30-250 ka
Qia3		middle Pleistocene	crowned	strong	strong	30-250 ka
Qoa	Qoa	mid-early Pleistocene	whaleback	strong, often stripped	secondary to none	500-800 ka

Table 2. Summary of alluvial fan unit nomenclature and corresponding surface characteristics from the chronostratigraphic framework of Menges and Miller (2007). For the scope of this study, the map unit designations of Miller and Menges (2007) were simplified to include two fewer units. The modified nomenclature used in this study (second column) is shown in comparison to corresponding map units of Miller and Menges (2007).

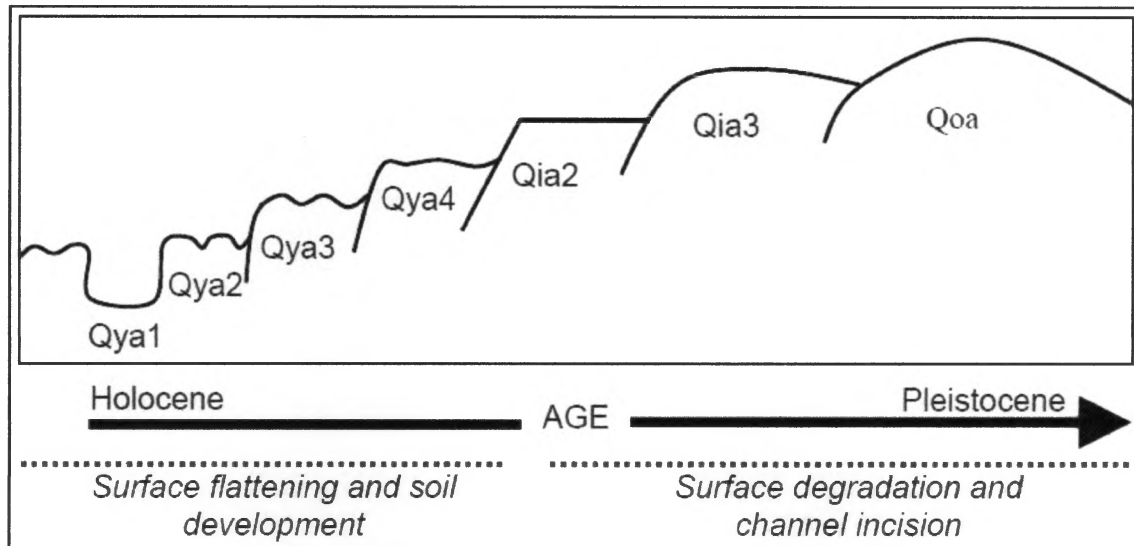


Figure 5: Illustration of progressive development of surface morphology for alluvial fan units based on chronostratigraphic framework by Menges and Miller (2007). See Table 1 for associated surface characteristics. Figure from Green (2009).

### 3.2 Clast Counts

Clasts counts were conducted at ten locations to determine clast composition of representative conglomerate units within the NHF (Table 1; Plate 1). The method used follows Howard's (1993) ribbon method. With exception that the number of clasts that were counted was limited to 100 per site. Clast lithologies were identified as hand specimens with the aid of a 10x hand lens and binned into six types and plotted in Excel (Figure 18). Count data are provided in Appendix I.

### 3.3 Tephrochronology

Two tephra samples obtained from the Noble Hills Formation were analyzed for their major earth element characteristics by the U.S.G.S Tephrochronology Lab in Menlo Park, California. Lab reports showing statistical correlation coefficients for the closest matches to other tephra samples in the Tephrochronology Lab data base and report narratives explaining the lab results are provided in Appendix II. Sample locations are shown on Plate 1.

Sample JC-NH06-T1 was collected by J. Caskey (SFSU) in January 2006, prior to the initiation of this study. Correlation of this tephra to the 3.34 Mesquite Springs tephra (E. Wan, U.S.G.S., written comm.; Appendix II) was critical for constraining the age of the uppermost members of the Noble Hills Formation and placing a maximum limiting age for the onset of northeast-vergent contraction in the Noble Hills.

A second tephra sample, JN-NH-121102 T590-2, was submitted for lab analyses (Appendix II). This tephra matched most closely to several Quaternary tephra samples in the tephra data bank (Wan, E., written communication, 2013; Appendix II). This age is viewed as unreasonable given the structural and stratigraphic context of the strata that the sample was collected from, and has not been used to constrain the age of the constituent deposits

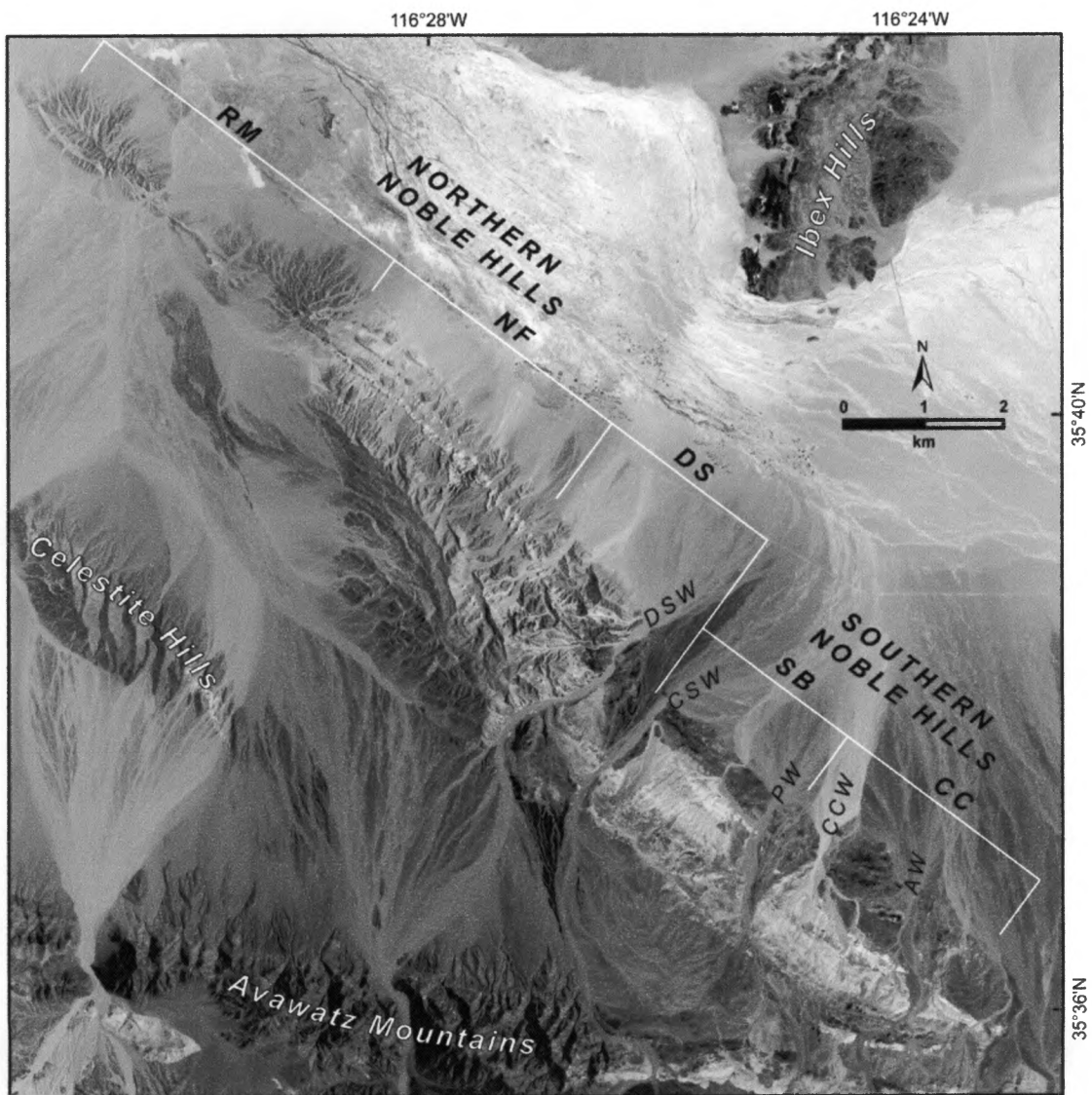


Figure 6: Index map of the Noble Hills showing the locations of specific washes and different areas of the referred to in the text. Abbreviations used: AW—Amphitheater Wash, CC—Canadian Club area, CCW—Canadian Club Wash, CSW—Cave Spring Wash, DS—Denning Spring area, DSW—Denning Spring Wash, NF—Niter Field area, PW—Pipeline Wash, RM—Round Mountain section, SB—Salt Basin area.

#### 4.0 STRATIGRAPHY

The rocks and sediments of the Noble Hills range in age from Proterozoic to Quaternary; rocks consist of sedimentary, metamorphic and igneous types (Troxel and Butler, 1979). Neogene basin sediments outcrop along the entire length of the Noble Hills. In the southern part of the Noble Hills the Neogene deposits are separated into two areas by a northeast and southwest by a northwest-trending “axial crystalline ridge” (Brady, 1984, 1986a) herein referred to more simply as the axial ridge. The axial ridge comprises Precambrian Crystal Springs Formation of the Pahrump Group (pC<sub>u</sub>, plate 1), which is locally intruded by 1.1 Ga diabase sills, and Cretaceous(?) granitoids referred to differently in the literature as both quartz monzonite (Butler and Troxel, 1979) and leucocratic adamellite (Stamm, 1981) (Mzla - Mesozoic leucocratic adamellite, plate 1). The adamellite presumably intruded at or near the depositional base of the Crystal Springs Formation, which is regionally expressed as the “great” nonconformity with underlying Precambrian cratonal rocks. This follows because the intrusive contact between the Crystal Springs Formation and the adamellite exhibits common pendants of cratonal schist and gneiss (Troxel and Butler, 1979) (pC<sub>gn</sub> – gneiss, plate 1). Brady (1986a) noted differences in the overall lithologic character of Neogene strata found on the northeast and southwest sides of the axial ridge and he distinguished these packages of strata as the *eastern* and *central* belts (Figure 4), respectively, and interpreted the two belts as representing basin deposits of different ages. In this report, the entire *eastern belt* of Brady (1986a), together with at least part of his *central belt* are interpreted as

belonging to an essentially conformable assemblage of Pliocene basing deposits, informally referred to herein as the Noble Hills Formation (NHF). The depositional history and subsequent tectonic history of the NHF are the primary focus of this investigation. A brief overview of the Noble Hills basin below is followed by detailed descriptions of the seven informal members (i.e., mappable subunits) recognized for the NHF.

#### **4.1 Noble Hills Formation**

The NHF is well exposed along the entire length of the Noble Hills (Plate 1). The northwest-striking and commonly steeply northeast dipping strata of the NHF define the structural grain of the Noble Hills. Aside from some of the more dramatic structural complexity found in the southernmost Noble Hills, aerial images of the Noble Hills as viewed with an up-to-the-northeast orientation provide a fairly representative cross sectional perspective of the basin strata that make up the NHF. The formation is a heterogeneous assemblage of interbedded and locally interfingering strata that is comprises interbedded fine-grained clastic and evaporitic rocks and sediments, alluvial conglomerates, minor limestone, and megabreccia (i.e., rock avalanche/slide deposits). One particular unit of reddish-brown, halitic mudstone (nh1c) is laterally continuous along most of the trend of the Noble Hills. Conglomerate makes up roughly 30-50% of the NHF. Packages of conglomerate and interbedded finer-grained clastic sediments and evaporates are notably discontinuous within the Noble Hills basin. Additionally,

conglomerates exhibit notable differences in their clast lithology assemblage types along the length of the Noble Hills. This perhaps reflects different sources feeding into alluvial fan system that may have prograded in from the margins of the basin from different directions. Alternately, prior interpretations of large-magnitude dextral offsets in SDV require that full consideration is also given to tectonic transport as a potential mechanism for variations in provenance observed within the Noble Hills basin.

The strata of the NHF are herein divided into seven mappable subunits (Figure 7; Plate 1) based on lithologic differences and relative stratigraphic position. The correlation of NHF map units in Figure 7 displays the lateral stratigraphic relations.

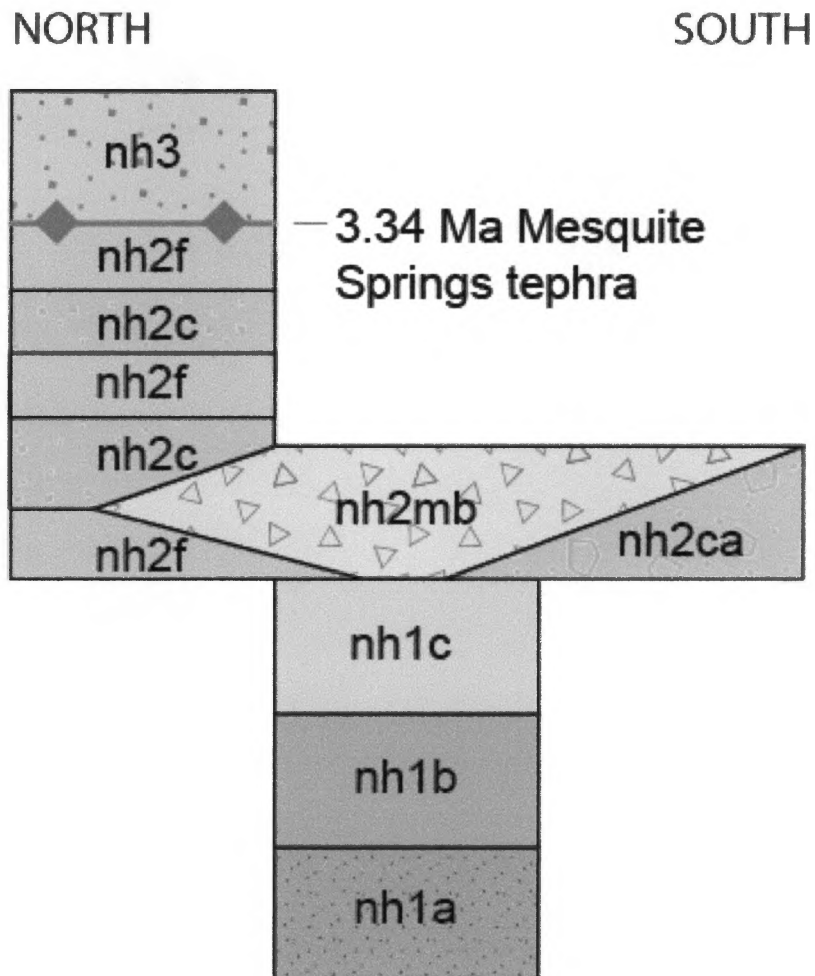


Figure 7: Correlation of units of the Noble Hills Formation showing lateral stratigraphic relations of the nh2 units. See Plate 1 for full correlation of map units.

#### ***4.1.1 nh1a – Lower Sandstone and Siltstone Member of the Noble Hills Formation***

The lowest exposed stratigraphic unit, nh1a, is a well-bedded, poorly-indurated, generally fining-upward sequence consisting of vari-colored arkosic sand, matrix-supported fine-pebble conglomerate, fine-grained sandstone, siltstones, and conspicuous, well-indurated limestone, and gypsum. The nh1a member varies from brown, tan, light-

red, light-gray, light-green, pink to white. The nh1a strata are predominantly thin-bedded, but locally medium-bedded. Finer grained beds are most commonly thinly laminated. Graded bedding, troughs, and trough cross-beds are common in sandstone and siltstone facies (Figure 8). Limestones intervals display crenulated laminations, crystalline texture, and secondary laminar and nodular chert (Figure 8). Limestone in the Canadian Club Wash area serves as a distinctive marker bed (Figure 8,) that is traceable along strike for some distance. Additionally, this limestone marker bed facilitates structural reconstruction of the highly deformed strata.

In the southern part of the Noble Hills the lowermost exposed strata of nh1a appear to be everywhere in contact with Crystal Springs Formation along the axial ridge fault (Plate 1). However, locally along this contact nh1a strata appear to lie depositionally on the Crystal Springs Formation. In the northern part of the Noble Hills, the base of nh1a is not exposed. Estimates of the stratigraphic thickness of nh1a are problematic because the unit is most commonly in fault contact with other units in either the upper or lower part of the unit, or both, and because this unit is commonly highly folded. However, map relations in the in the Canadian Club Wash area (Figure 6; Plate 1) indicate that nh1a is at least 100 m thick.

The sandstone and pebble conglomerate facies of nh1a are interpreted to have been deposited in marginal lacustrine sandflats in a marginal lacustrine environment (Miall, 1977). Fluctuation in grain-size and presence of shallow trough cross-bedding likely reflects changes in proximity to the distal ends or toes of alluvial fans. Interbedded

siltstone and gypsum evaporites were likely deposited along the margin of a fluctuating ephemeral lake margin or saltpan. Trough cross-bedding likely represent episodes of fluid flow into the basin during period where standing water was present. Similarly, normal-grading present in coarser sandstone facies represent distal debris flow events entering shallow, standing water. Limestone may represent a marshy spring environment at the margin of a saline lake.

#### **4.1.2 *nh1b – Gypsiferous Member of the Noble Hills Formation***

The nh1b member consists of light grayish-white to light greenish-white evaporitic gypsum, and minor reddish brown siltstone. The unit is commonly highly-folded, and exhibits conspicuous mylonitic foliation where gypsiferous units are sheared by plastic flow in the vicinity of thrust faults. One of the best and most accessible exposures of gypsiferous mylonites is in the dry waterfall areas where the unit forms the hanging wall of the Canadian Club thrust in the Canadian Club Wash area (Figure 6: Index map of the Noble Hills; Section 5.1). Where highly-folded, fold orientations are often kinematically discordant to the adjacent or nearby thrusts, suggesting somewhat nonsystematic deformation that likely relates to the highly plastic behavior of the gypsiferous interval. Where highly strained, and especially in the southern Noble Hills, gypsiferous intervals contain thin (up to a few-mm-thick) secondary manganese oxide layers that are deformed into distinct boudinage structure (Figure 9). Original thickness of nh1b likely varies naturally owing to its evaporitic origin, although determining thickness of this member is difficult because of its severely attenuated and tightly folded character in most areas

where it is well exposed. Where upper and lower bounding stratigraphic contacts of nh1b are exposed in the Salt Basin area (Figure 12A, 7B), the approximate structural thickness is estimated to be 150 m.

The interbedded evaporite and siltstone of nh1b is interpreted to have been deposited in a saline mudflat environment marginal to an ephemeral saline lake (Miall, 1977).

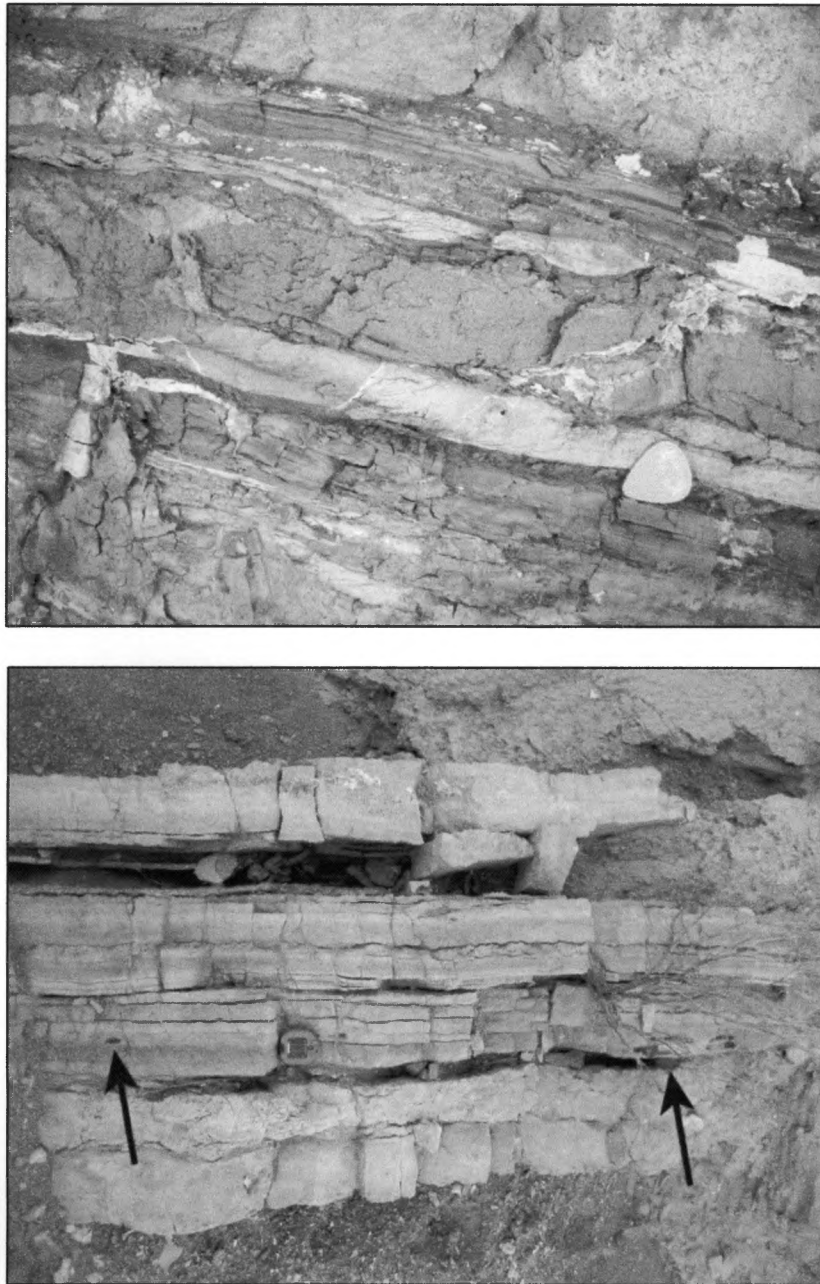


Figure 8: Sedimentologic characteristics of the lower sandstone and siltstone member of the Noble Hills Formation (nh1a) in the Canadian Club Wash area (Figure 6: Index map of the Noble Hills). Upper photo shows thinly laminated and planer bedded fine-grained sandstones and siltstones and trough cross-bedding in light gray layer to the left of the guitar pick; white gypsum is secondary (guitar pick for scale - long axis is 3 mm). Lower photo is of limestone marker beds found within nh1a. Note crenulated lamination and secondary chert nodules (arrows). Brunton compass for scale.



Figure 9: Highly sheared mylonitic gypsum within nh1b member, with layers of strongly attenuated secondary manganese oxide (black). The relatively more competent manganese oxide intervals display boudinage structure.

#### ***4.1.3 nh1c – Halitic Mudstone Member of the Noble Hills Formation***

Unit nh1c consists of reddish-brown halitic muds and silts. Bedding is mostly absent in exposures. The halite bearing muds and silts of nh1c are weakly to moderately indurated; where halite is concentrated, the unit is highly indurated. The unit is poorly exposed except where massive, crystalline halite is exposed (Figure 10) by in the vicinity

of mining excavations at Salt Basin and Jumbo Deposit in the southern Noble Hills. These massive halite deposits likely represent concentrations formed by the dissolution and reprecipitation of halite from the surrounding halitic mudstone. Halitic mudstones are distinguishable in the field by taste, vertical flute-style weather, and hummocky, small-scale karst topography of slopes formed on the unit. In the northern Noble Hills, the unit is distinguished by an along-strike alignment of relatively resistant, reddish-brown, rounded hills (Figure 11). In the southern Noble Hills, nh1c contains minor exposures of well-bedded sandstone, and sparse sub-angular pebble conglomerate. Minor pebble-conglomerate found sporadically interbedded within the nh1c member in Salt Basin area contains similar lithologies as the overlying nh2c conglomerates (i.e., diorite and quartzites). Within the upper nh1c exposed in the Salt Basin area, contorted beds of sandstone and siltstone are present, and are presumably a transitional facies between nh1c and nh2c members.

The basal contact of nh1c is best exposed in the southern Noble Hills in the Salt Basin area, where it is in sharp depositional contact with the underlying gypsum of nh1b (Figure 12B). Although bedding in the nh1c is poorly exposed in the field, it is easily distinguished by its dark reddish brown color, distinctive small-scale karst topography on slopes formed on the unit, locally thick, pure, halite masses, and in the northern Noble Hills by the conspicuously high, reddish-brown, round-topped, steep-sided, alignment of hills (nh1c, Figure 11).

The halitic mudstone of nh1c is interpreted to have been deposited on a saline mud flat, based on the lack of primary sedimentary structure (Miall, 1977).



Figure 10: Massive, crystalline halite ~300 m northwest of Amphitheater Wash in nh1c. Note vertical dissolution flutes. Massive halite is a product of reprecipitation of dissolved and migrated NaCl from surrounding mudstone, so the white bands near the center of the photo are secondary features formed within the massive halite.

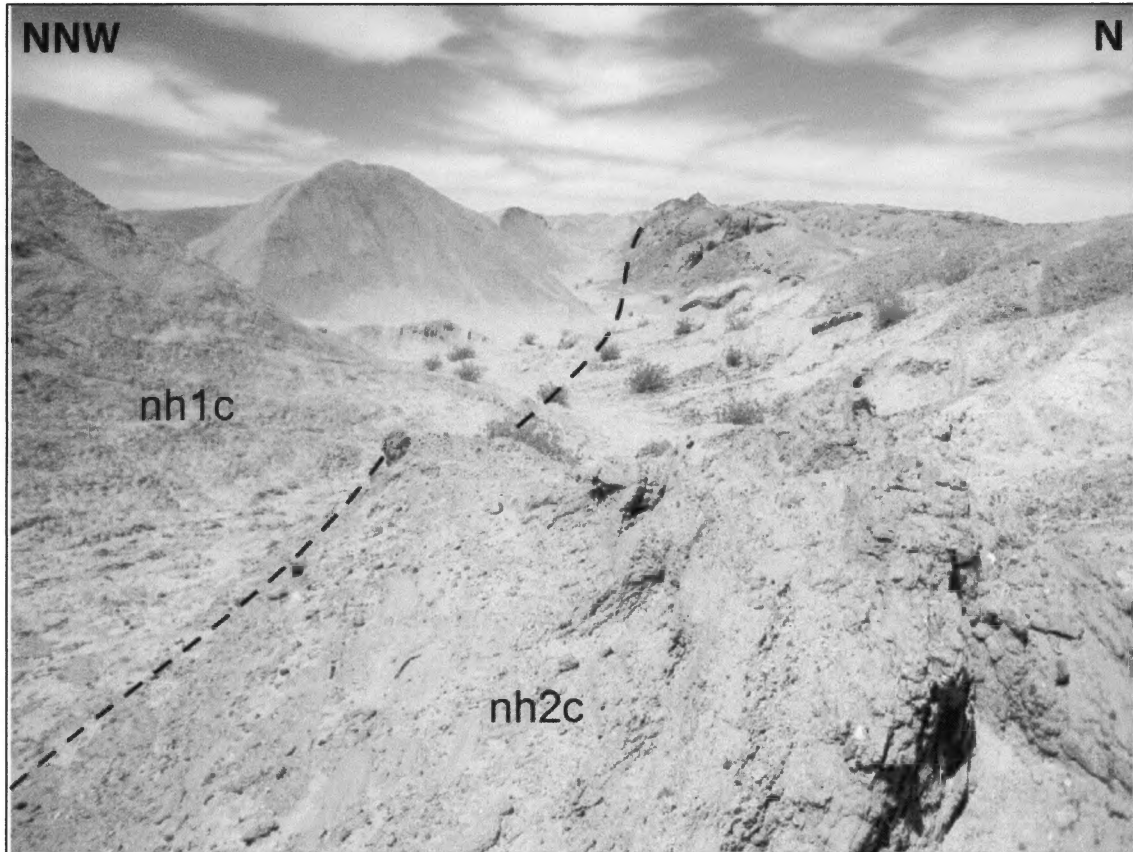


Figure 11: Contact between nh1c and nh2c in the Niter Field area. Reddish-brown halitic silts of nh1c form prominent ridges approximately 10-15 m in height. Conglomerate of nh2c is sub-vertical to overturned in this exposure.

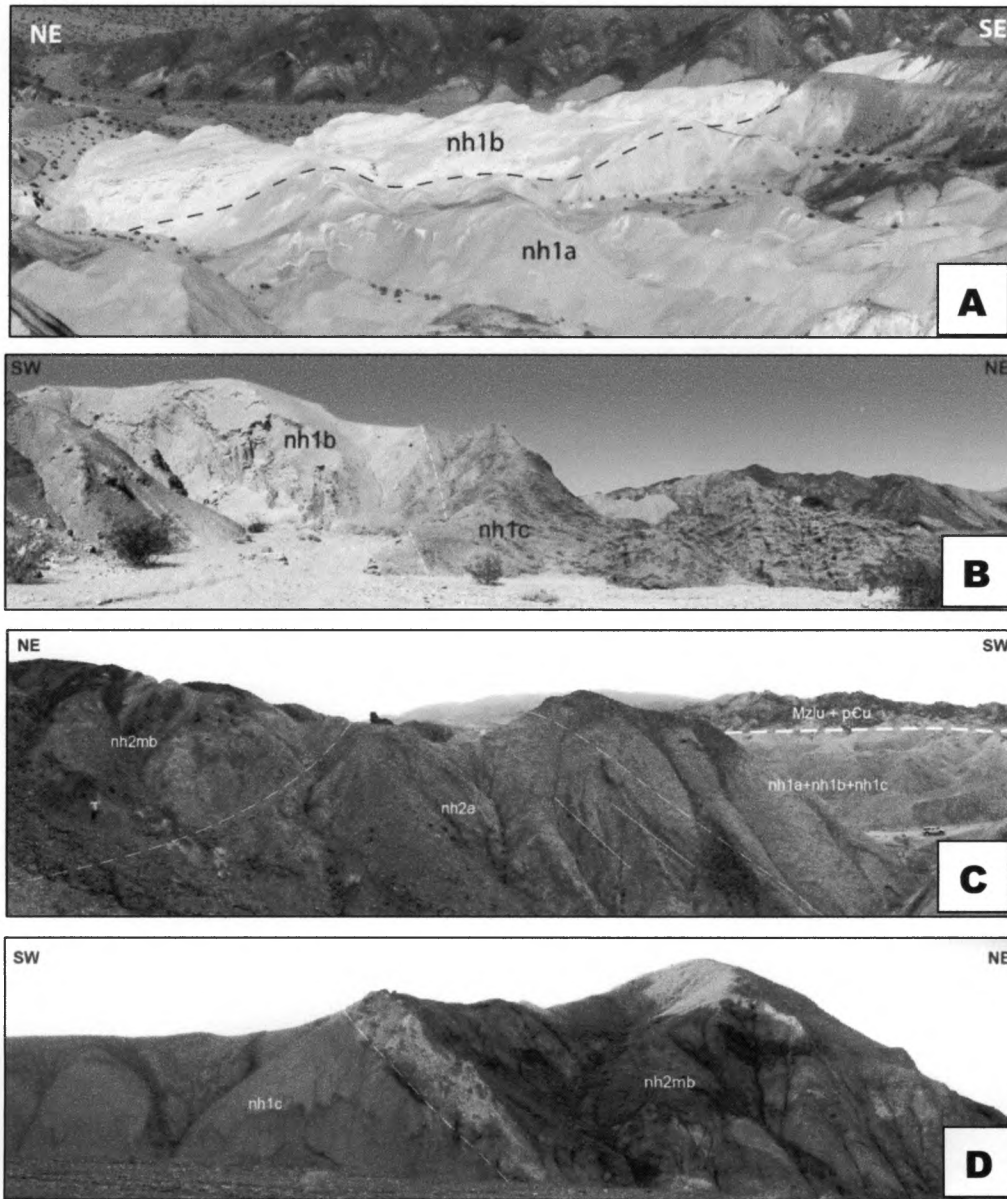


Figure 12: Representative contacts between members of the NHF. Photo A (view east from axial ridge) shows contact between the sandstone and siltstone of nh1a and the gypsiferous nh1b in the Salt Basin area. Photo B (view northwest) shows depositional contact (dashed white line) between gypsiferous nh1b (left) and halitic nh1c (right) in the Salt Basin area; note hummocky dissolution weathering in nh1c, and NE dipping bedding in nh1b. Photo C (view southeast) shows contacts between the halitic nh1c, conglomeratic nh2c, and megabreccia nh2mb units; solid white lines depict bedding planes. Photo D (view northwest) shows moderately northeast-dipping depositional contact (dashed white line) between halitic nh1c and nh2mb megabreccia exposed on the north side of Pipeline Wash (Figure 6).

#### **4.1.4 *nh2c and nh2ca – Conglomerate Member of the NHF***

Conglomerate identified as nh2c is present along nearly the entire length of the Noble Hills; however, variations in constituent clast lithologies, size and rounding, and unit thickness occur laterally. Based on these mappable differences, the sub-designation “a” has been added to deposits consisting of exclusively Avawatz Mountains-sourced lithologies (i.e., nh2ca), so as to distinguish them from deposits containing lithologies from multiple-sources.

The nh2ca conglomerate is mapped exclusively in the southern Noble Hills (plate 1) and is locally well exposed in wash cuts; elsewhere it tends to be covered by gravel lag deposits derived from the same unit, which is easily distinguishable by its very dark, nearly black color on aerial images. The unit consists of poorly-bedded, mostly matrix supported, angular to sub-angular, pebble-to-cobble conglomerate containing clasts of quartzite, limestone, marble, and diorite, with lesser clasts of gneiss and schist (Figure 13; Figure 18, CCNH004). Conglomerate is interstratified with well-bedded fine-grained deposits of fine-to-pebbly sandstone, mudstone, and gypsiferous evaporite.

The nh2ca unit generally fines and thins northwest of the Canadian Club Wash area where it is interbedded with pebbly sandstone, mudstone, and evaporites, which are somewhat similar in character to those in nh1a. Prevalent throughout the nh2ca are distinctive clasts of recrystallized diamictite facies of the Kingston Peak Formation, banded siltstone of the Crystal Spring Formation, diorite, monzodiorite, whitish and pinkish quartzite, and granitic gneiss. Where exposed in the southern Noble Hills, the

basal contact with the halitic mudstone of nh1c is conformable and gradational (Figure 11, (Figure12B). This is supported by the minor conglomerate channels or intervals identical in composition to Avawatz sourced gravels that are interbedded with the halitic mudstone (nh1c) in the Salt Basin area.

Given the lateral variation in facies, the nh2ca is interpreted to have been deposited in a mid-fan to lake margin environment. The cyclical nature of the deposits suggests multiple debris flow events being deposited in an ephemeral lake environment. Where the nh2ca conglomerates are thickest between in the Amphitheater Wash area (Figure 6: Index map of the Noble Hills), the deposit is interpreted to be entirely deposited by debris flow events in a mid-fan depositional environment. The observations that the nh2ca strata are dominated by coarse, angular debris flow deposits consisting entirely of Avawatz Mountains-derived lithologies, and that the unit presently occupies a position at the base of the Avawatz Mountains, strongly support the interpretation that this unit is essentially in situ.

Exposures of nh2c in the northern Noble Hills are moderately-to-well-bedded, sandy matrix-supported, sub-rounded to angular, pebble-to-cobble conglomerate (Figure 14). Presence of quartzite, carbonate rocks, and diorite in the northern exposures (CCNH010, Figure 18) strongly suggests an Avawatz Mountains source. The presence of granitic clasts in the northern exposures suggests an input from Owlshhead Mountains. As the nh2c and nh2ca strata are stratigraphically equivalent deposits, the deposits are

interpreted together as a proximal fan prograding out onto an ephemeral marginal lake environment.



Figure 13: Avawatz-sourced conglomerate member (nh2ca) exposed in the Canadian Club Wash area. Note poor bedding, and sub-angular clasts. Photograph is of clast count location CCNH004 (Figure 18). Clipboard for scale.

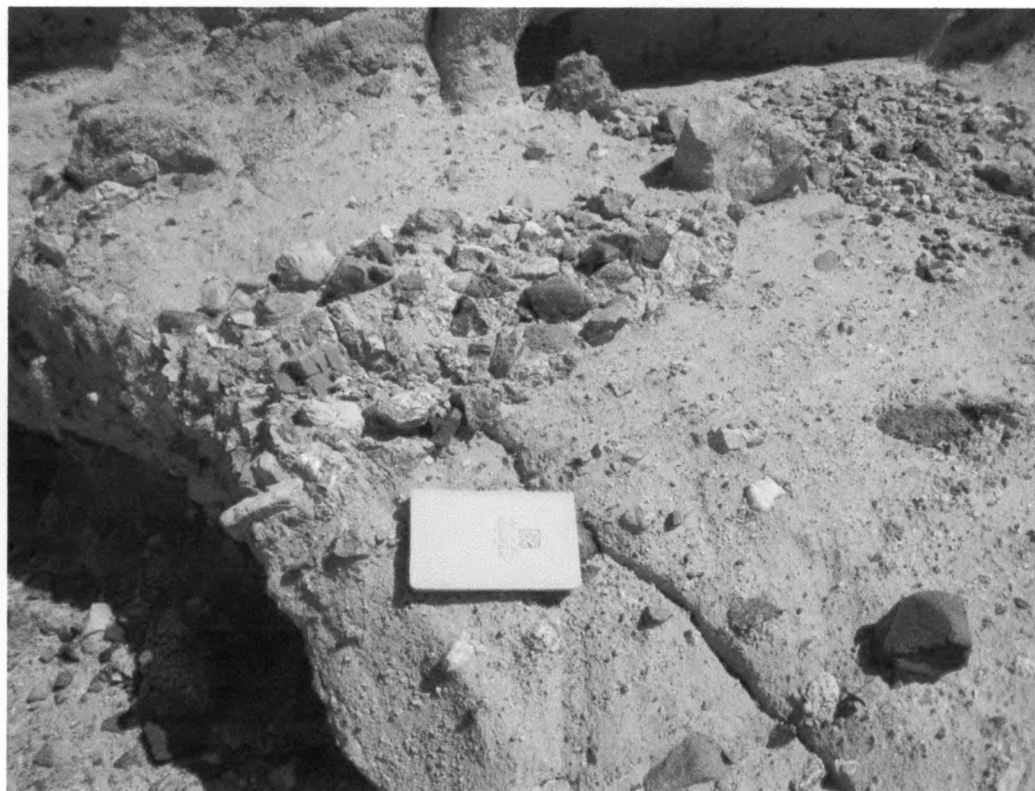


Figure 14: Mixed lithology conglomerate (nh2c) exposed in the Niter Field area. Field book for scale.

#### ***4.1.5 nh2f – Upper Sandstone, Siltstone and Gypsiferous Member of the NHF***

Only mapped in the northern Noble Hills, nh2f consists of well-bedded, siltstone, sandstone and gypsiferous member. In the Niter Field area, nh2f outcrops in two laterally discontinuous packages that are conformable to, and stratigraphically alternate with conglomerates of nh2c. The upper contact is conformable with the granite-bearing conglomerate of nh3. Interbedded with nh2f is a tephra layer that is correlated to the 3.34 Ma Mesquite Springs Tephra (JC-NH06-T1, Appendix II). This tephra layer is

concordant to nh2f strata in the Niter Field area (Plate 1) and can be traced to the northwest where it becomes concealed beneath an angular unconformity marking the contact between nh2f and the younger fanglomerate of Tf3 (Figure 17).

Given the similarity to the nh1a member, nh2f is interpreted to have been deposited in a marginal ephemeral lacustrine environment.

#### **4.1.6 *nh2mb – Megabreccia Member of the NHF***

Member nh2mb consists entirely of megabreccia (i.e., bedrock derived landslide deposits) that outcrops along the northeast edge of the southern Noble Hills (Plate 1). The megabreccia deposits are the youngest exposed stratigraphic unit of the NHF south of Denning Springs Wash (Figure 6, Plate1). Lithologies present within the megabreccia were not mapped in detail. This deposit consists of pervasively fractured, locally brecciated, and chaotically broken and reassembled blocks derived from Proterozoic granitic gneiss, the Kingston Peak and Crystal Springs formations of the Proterozoic Pahrump group, younger Proterozoic Johnnie Formation and Stirling Quartzite, and Mesozoic granitic and dioritic rocks. The identification of bedrock source lithologies were guided, particularly in the early phases of the field study, by original unpublished field maps (circa, 1977) of B. Troxel. Of particular note, the various lithologies found in the nh2mb megabreccia appear to be identical to the clast type assemblages found in the underlying nh2ca conglomerates found in the southern Noble Hills (Figure 13).

Individual block sizes are highly variable and difficult to estimate, but are commonly tens of meters across. In the Canadian Club Wash area (Figure 6Figure 6: Index map of the

Noble Hills), nh2mb depositionally overlies conglomeratic and fine-grained facies of nh2ca. In the Salt Basin area (Figure 6), nh2mb depositionally overlies halitic mudstone of nh1c (Figure 12D) as well as locally present nh2c conglomerate. The basal contact is best exposed along the northwest channel wall of Pipeline Wash (Figure 6) where the contact dips  $\sim 45^\circ$  NE, concordant to underlying laminated beds of sandy halitic mudstone. The basal contact of the megabreccia is marked by a conspicuous  $\sim 1$  meter thick, dark zone containing pulverized rock fragments intermixed with fine-grained material, which displays a contact-parallel fabric. As nh2mb lacks internal sedimentary structure, determining stratigraphic thickness of nh2mb is problematic. However, the across-strike map width of nh2mb reaches a maximum of  $\sim 800$  meters near the mouth of Canadian Club Wash, which is considered a maximum exposed thickness of the nh2mb megabreccia deposits.

The nh2mb megabreccia deposit is interpreted to have been derived from the proximal Avawatz Mountains to the south and southeast of the Noble Hills, based on numerous observations. The dark, strongly recrystallized, granite and gneiss bearing diamictite of the Proterozoic Kingston Peak Formation present in nh2mb represents the southern facies of the Kingston Peak Formation that is found to the south of a northwest-trending line that extends through southern Death Valley (Troxel, 1967). While the southern facies of the Kingston Peak Formation outcrops in southern Death Valley at the southernmost tip of the Saddle Peak Hills (Troxel, 1982) (Figure 3), in the Southern Salt Spring Hills (Troxel, 1967) (Figure 3), exposures along the northeasternmost edge of the

Avawatz Mountains at the mouth of Sheep Creek Wash (Troxel and Butler, 1979) are the most petrologically similar. Additionally, Troxel and Butler (1979) mapped Crystal Springs Formation at Sheep Creek Wash. Dioritic and granitic lithologies in nh2mb bear close resemblance to the lithologies found in the Mesozoic Avawatz quartz monzodiorite complex that outcrops extensively in the Avawatz Mountains, and intrudes all metasedimentary rocks in the range (Spencer, 1981). Spencer (1981) mapped remnants of Johnnie Formation in the central Avawatz Mountains and Stirling Quartzite in the central and southern Avawatz Mountains. Additionally, field reconnaissance conducted as part of this study examined sedimentary breccia deposits with strikingly similar lithologies (e.g., gneiss, dark, recrystallized Kingston Peak Formation diamictite) interbedded within the Avawatz Formation of Spencer (1981, 1990b) high in the central Avawatz Mountains. In summary, the Avawatz Mountains source interpretation is strongly favored here, as a source area containing a similar suite of lithologies is not found to the north or east.

Troxel and Butler (1979) documented that the Precambrian sourced lithologies within the nh2mb deposit are in reverse stratigraphic order, indicating progressive denudation of the source during one or more landslide events associated with tectonic oversteepening of the Avawatz Mountains along a rangefront fault, although it is unclear from their report which direction they interpreted as being stratigraphically up. The Avawatz Mountains source interpretation is strongly favored here, as a source area containing a similar suite of lithologies is not found to the north or east. Given the assumed catastrophic nature of the nh2mb deposits, the deposit is inherently proximal to

its source area. As the basal contact of the member changes laterally from the conglomerates of nh2c in the Canadian Club Wash area to the halitic silts of nh1c in the Salt Basin area (Plate 1), the deposit likely ran out onto the margin of a saline lake, fringed by alluvial fans represented by nh2ca conglomerate in the southern Noble Hills.

#### **4.1.7 nh3 – Granite Bearing Conglomerate of the NHF**

The nh3 conglomerate member is a poorly-bedded, pebble-to-boulder matrix-supported conglomerate and interbedded sandstone (Figure 16). Clasts within nh3 are predominantly granitic, with minor volcanics rocks and quartzite (CCNH008 and CCNH009, Figure 18) in a coarse-grained sandy matrix. These deposits are confined to the upper strata of the northern Noble Hills. In the Niter Field area, tephra correlated to the 3.34 Ma Mesquite Springs tephra (JC-NH06-T1, Appendix II) is interbedded with nh3 strata. This layer of tephra can locally be seen crossing the contact between nh3 and the underlying nh2f (Figure 15), strongly supporting the conformability on the two members. Where exposed at Denning Spring Wash (Figure 6), the thickness of nh3 is at least 150 m.

The nh3 member is a debris flow facies that has previously been interpreted to have been deposited in a mid-alluvial fan environment (Brady, 1986a, 1986b) on the east side of the Owlshead Mountains, and subsequently tectonically transported to its present position in the Noble Hills. Although similar granitic rocks are found to the southeast of the Noble Hills in the northern Salt Spring Hills and as an inselberg of intact granite on the Avawatz Mountain piedmont, the Owlshead Mountain source for these deposits is

avored given the abundance and appearance of granite, as well as the presence of volcanics, and quartzite.

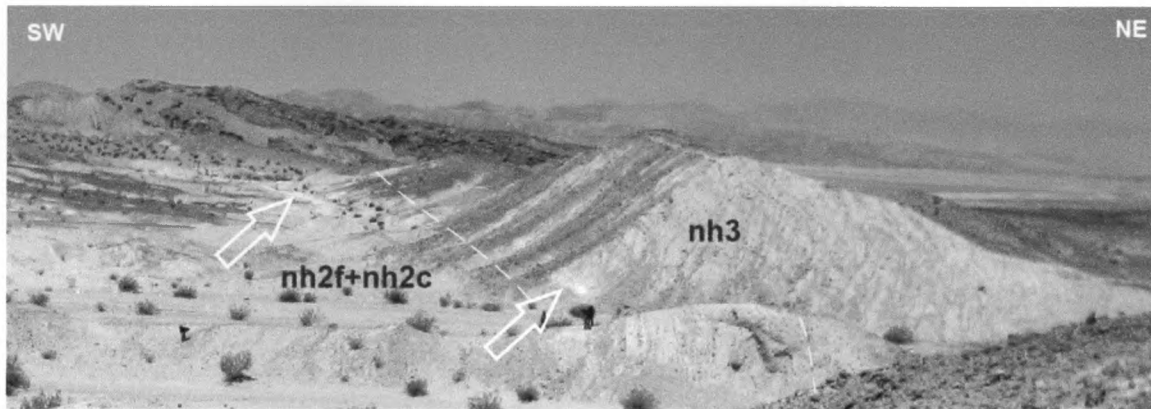


Figure 15: View of Niter Field area showing contact (dashed white line) between the granite bearing conglomerate (nh3) and older sandstone of nh2f; direction of view is approximately on strike with bedding of both units. Arrows point to discontinuous beds of the Mesquite Springs tephra found within units nh3 and nh2f. Right arrow points to sample location of JC-NH06 (Plate 1; Appendix 2).



Figure 16: Granite bearing conglomerate (nh3). Outcrop in the Denning Spring area showing pebble-to-cobble conglomerate and interbedded sands. Strata dips to the northeast. Rock hammer for scale.

## 4.2 Tertiary Fanglomerates

Nomenclature for the Tertiary fanglomerates is based on the relative depositional relationship to Pliocene strata and other fanglomerate units; they are, from oldest to youngest, Tf1, Tf2, and Tf3. Present along the length of the Noble Hills, Tf3 is the most abundant fanglomerate unit in the map area (Plate 1), with exposures occupying the highest topography in the Noble Hills.

Tertiary fanglomerates are present along the length of the Noble Hills, where they unconformably overlie or are otherwise inset into strata of the NHF (Figure 17). The age of these deposits is not well constrained; however, they overly previously deformed Pliocene strata of the NHF, as well as older strata of central belt of Brady (1986a) and have themselves been uplifted and broadly deformed by folding and minor faults, particularly along the margins of the units. Clast counts of the Tf3 conglomerate conducted at three locations (CCNH002, CCNH003, and CCNH006, Figure 18) suggest that these deposits have a source in the Avawatz Mountains, based on the presence of diorite in all distributions and volcanics the CCNH003 and CCNH003 distribution; the gneiss and granitics of CCNH006 (Figure 18) are interpreted to have been reworked clasts derived from the proximal Military Canyon Formation exposed along the northern edge of the Avawatz Mountains (Plate 1). The fanglomerates of Tf1 through Tf3 were deposited in upper-to mid-fan depositional environments. Tf1 and Tf2 are interpreted as being deposited in channels eroded into the NHF strata.

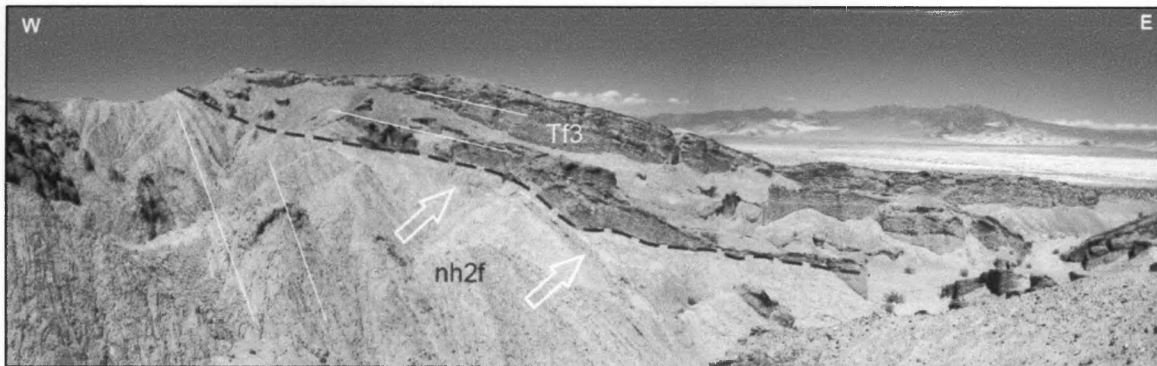


Figure 17: View to the north of the contact (dashed black line) between capping fanglomerate Tf3 and upper sandstones and siltstones of Noble Hills Formation (nh2f), showing angular unconformity and white layer of tephra (white arrows) in nh2f member of the Noble Hills Formation. Solid white lines depict approximate dip of bedding planes. Tephra has not been correlated to the Mesquite Springs tephra, but beds exposed here can be traced along strike to the JC-NH06 sample location seen in Figure 15.

### 4.3 Quaternary Alluvium

Alluvial fan deposits are extensively exposed in the Noble Hills piedmont, as well as within the numerous channels cutting perpendicular to the structural grain of the Noble Hills. The extensive nature of these deposits made field determinations impractical, thus relative stratigraphic position has largely been assigned based on surface characteristics evaluated using color aerial photographs. Unit designations are modified from Menges and Miller (2007).

#### 4.3.1 *Qoa – Middle-Early Pleistocene Alluvial Fan Deposits*

Qoa deposits are located in the southern Noble Hills in Pipeline Wash (Figure 6). Deposits are deeply dissected, and display linear whaleback-ridges (Table 1). Qoa deposits contain distinctly Avawatz Mountains sourced diorite and metasedimentary

rocks, as well as volcanic and granitic rocks likely reworked from the proximal Military Canyon Formation (CCNH005, Figure 18). According to the chronostratigraphic framework by Menges and Miller (2007), Qoa deposits are 800-500 ka.

#### ***4.3.2 Qa2 – Middle Pleistocene Alluvial Fan Deposits***

Qa2 deposits are distributed throughout the map area (Plate 1) and found at relatively higher elevations than younger alluvial deposits. Surfaces contain well varnished clasts and strong desert pavement, and are easily identified in aerial imagery by their dark tone. Where Qa2 deposits are laterally extensive, they are moderately dissected with flat to crowned surfaces. According to the chronostratigraphic framework by Menges and Miller (2007), Qoa deposits are 250-30 ka.

#### ***4.3.3 Qa1 – Late Pleistocene Alluvial Fan Deposits***

Qa1 deposits are found throughout the map area (Plate 1) and are either preserved well above active channels in highly dissected areas of the Noble Hills (e.g., the Canadian Club Wash area, Figure 6) or as abandoned fan surfaces. Surfaces are generally flat and exhibit moderate desert varnish and weak to moderate desert pavement. According to the chronostratigraphic framework by Menges and Miller (2007), Qoa deposits are 250-30 ka.

#### ***4.3.4 Qya3 – Middle Holocene Alluvial Fan Deposits***

Surfaces have pronounced bar and swale fan surface topography and are typically inset 10-60 cm below Qya4 surfaces. Qya3 surfaces contain weakly varnished clasts and

no desert pavement. There is a moderate amount of vegetation on the surface. Qya3 deposits are typically about 6-3 ka.

#### ***4.3.5 Qya2 – Late Holocene Alluvial Fan Deposits***

Qya2 deposits are the first surface above the active channels. Bar and swale fan surface topography is prevalent. Desert varnish and desert pavement are absent to weakly developed, and vegetation is abundant. Fan surfaces are considered active on centennial scales.

#### ***4.3.6 Qya1 – Late Holocene Alluvial Fan Deposits***

Qya1 deposits form the active to recently active channels. Deposits contain abundant bar and swale fan surface topography with no varnished clasts or desert pavement. Vegetation is abundant on Qya1 deposits. Qya1 deposits are readily identifiable in aerial photographs by their light color.

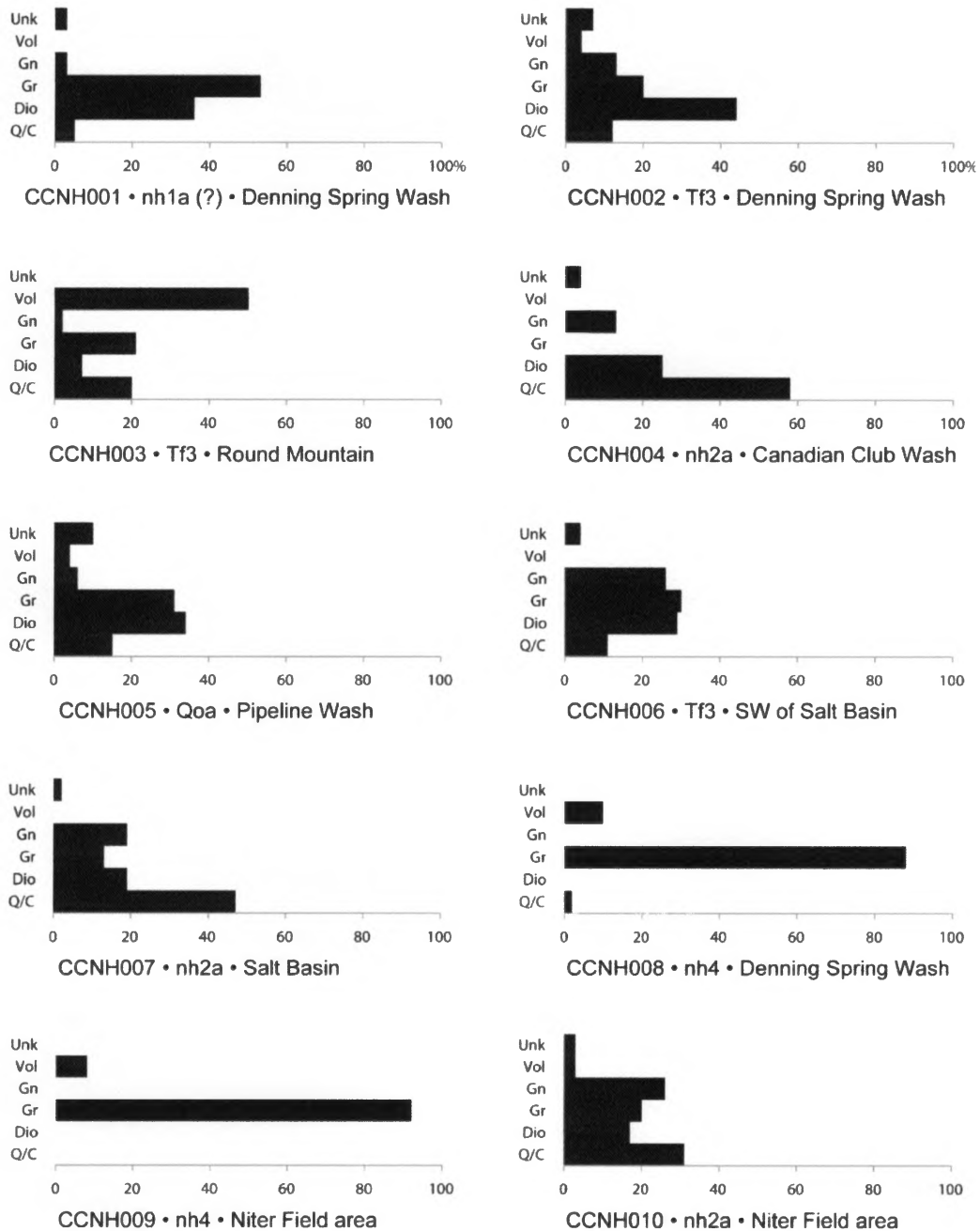


Figure 18: Histogram plots of clast composition percentages for conglomeratic units in the Noble Hills Formation. Lithologic abbreviations used: Unk – other or unidentified; Vol – Volcanic; G/S – gniess and schist; Gr – granitic; Dio – diorite; Q/C – quartzite (including Kingston Peak Fm. diamictite) or carbonate (limestone or marble). See Plate 1 for clast count locations.

## 5.0 STRUCTURAL GEOLOGY

The dominant structural style along the length of the Noble Hills is characterized by northeast-vergent contractional deformation involving all members of the Pliocene NHF. This deformation increases in intensity at the southeast end of the Noble Hills where they converge with the Avawatz Mountains and east-west striking strands of the Garlock fault system. Contractional deformation in the Noble Hills was recognized by earlier workers (Troxel and Butler, 1979; Stamm, 1981; Brady; 1984a, 1984b). The parallel nature of contractional structures to SDVFZ strands and the broadly accepted notion of a protracted history of large-magnitude slip on the fault zone logically led earlier interpretations that contraction was, in some sense, secondary to and coincident with the predominant dextral shear on the SDVFZ. This section presents a number of key field relations that indicate a much different tectonic history for the Noble Hills that includes an early (post-3.4 Ma) episode of intensive, northeast-vergent contraction that clearly predates the initiation of slip on SDVFZ, which encompasses fewer strands than depicted on earlier maps, and far lower estimates of net displacements. The following section first describes the style, magnitude, and timing of northeast-vergent folding and faulting along the length of the Noble Hills (Section 5.1). Section 5.2 then addresses the structural and stratigraphic relations that constrain the timing of amount of net displacement that has occurred on the SDVFZ in the Noble Hills.

## 5.1 Northeast Vergent Contractional Structures in the Noble Hills

Northeast-vergent deformation is strongly expressed within all strata of the NHF along the entire length of the Noble Hills. The contraction is consistently northeast-vergent although the character of the deformation varies from a relatively narrow belt of concentrated and extreme shortening in the CC Wash to Amphitheater Wash areas to a much broader belt that features overturned fault-propagation folds that involve nearly the entire stratigraphic thickness of the NHF. In the Canadian Club Wash area, the well-bedded sandstones and siltstones of nh1a form northwest-trending, overturned anticline-syncline pairs that are internally thrust along faults oblique to bedding (Figure 19). The overlying gypsum and siltstone of nh1b is more complexly folded and internally sheared; boudinage within the gypsum beds is common. Reliable estimates of shortening and structural relief are difficult to determine given the imbricate thrusting of fold limbs. However, based on measurements obtained from cross section data (Figure 19) the strata in the Canadian Club Wash area show a minimum of 100 m of shortening.

The CC thrust is exposed along the length of the southern Noble Hills (Figure 20). It is generally a sinuous, low angle fault that thrusts the gypsum of nh1b over conglomerate and fine grained units of nh2c from Amphitheater Wash to CC Wash and halites of nh1c, north off CC Wash. Where exposed, gypsum in the hanging wall of the CC thrust forms resistant escarpments and ridges (Figure 21). At Salt Basin and at the southern end of the CC Wash area, high concentrations of halite are present in the

footwall. The CC thrust is indicated on the Canadian Club Wash cross section (Figure 19). Net throw in the CC thrust is indeterminate and is likely variable along strike.

The axial ridge fault (ARF) (Figure 20) is a steep-to-vertical northwest-trending reverse fault that juxtaposes Precambrian and Cretaceous rocks of the axial ridge with Pliocene basin deposits of the NHF. This fault is poorly exposed at outcrop scale along its length, but its location and orientation can be inferred. Orientations on this fault are variable and range from maximum northeast dips of  $\sim 70^\circ$  in the Salt Basin area to maximum southwest dips of  $\sim 60^\circ$  to the north of Amphitheater Wash (Figure 6). This fault is described as the “central branch” of the SDVFZ by Troxel and Butler (1979), Stamm (1981), and Brady (1986a), with estimates of dextral displacement on the order of “as much as several miles” (Troxel and Brady, 1979). Where exposed near Amphitheater Wash, an approximately 1-2 m thick shear zone along the ARF is exposed (Figure 22); kinematic indicators within this shear zone are sparse, but observation of steeply oriented mullion axes strongly suggests an oblique, down-on-the-north component of motion. Conversely, where the ARF is exposed at the head of CC Wash, shearing is absent and bedding in the nh1a is concordant with bedding in the Precambrian Crystal Springs formation, and little to no shear along the inferred fault plane is apparent. In the Salt Basin area the existence of the ARF becomes questionable, given both the inferred northeast orientation of the contact between the axial ridge and nh1a, and observations in Denning Spring Wash suggest that the contact is depositional.

On the southwest side of the ARF, brittle deformation characterized by large-scale boudinage structures, and brittle shearing is prevalent within the Cretaceous granitic pluton and Precambrian roof pendants. Orientations of boudin axes were difficult to quantify, however, axes are generally subhorizontal to gently plunging. Additionally, mineralization indicative of hydrothermal alteration is present sporadically throughout the axial ridge, which suggests that the deformation of the rocks of the axial ridge predates deformation of the Pliocene strata of the NHF, as similar alteration is mostly absent from these strata.

In the Salt Basin area (Figure 6), the intensity of deformation exhibited by the nh1a member is considerably subdued relative to deformation on the CC Wash area. However, the overlying gypsum of nh1b is moderately to highly deformed here. While nh1b bounding contacts are visible in outcrop (Figure 12A & 12B), the complex deformation exhibited by nh1b obscures the upper contact along much its length in Salt Basin. The general nature of this upper contact is that the nh1b and nh1c members are in a faulted depositional contact, as the nh1b member forms a northeast-vergent, asymmetric anticline with a steep-to-overturned forelimb that has been breached by up-on-the-southwest thrusting. The observation is supported by the northwest projection of the Canadian Club Thrust (discussed in section 5.1.2) from Canadian Club Wash into Salt Basin (Figure 20, Plate 1).

Deformation of NHF strata in the northern Noble Hills is markedly less intensive. In the Niter Field area (Figure 6), deformation is generally characterized by steep-to-

overturned northwest-striking strata. Given the apparent conformability of units of the Noble Hills Formation from nh1a to nh3, as discussed previously (Section 4.1), the structural interpretation favored here is that they form the steep-to-overturned forelimb of a northeast-vergent fault-propagation fold. Based on measurements derived from the cross section (Figure 18), this fold has approximately 800 m of structural relief. The backlimb of the fold has been faulted along a right-oblique strand of the. An upper limit on the timing of deformation is given by the presence of the 3.34 Mesquite Springs tephra in the nh2f and nh3 strata. However, lower constrains are unclear. The capping Tf4 conglomerates which rest unconformably on the NHF strata are deformed (i.e., tilted) in a style compatible with the northeast rotation of the underlying forelimb strata involved in fault-propagation folding; however, constraints on the age of these deposits is unclear.

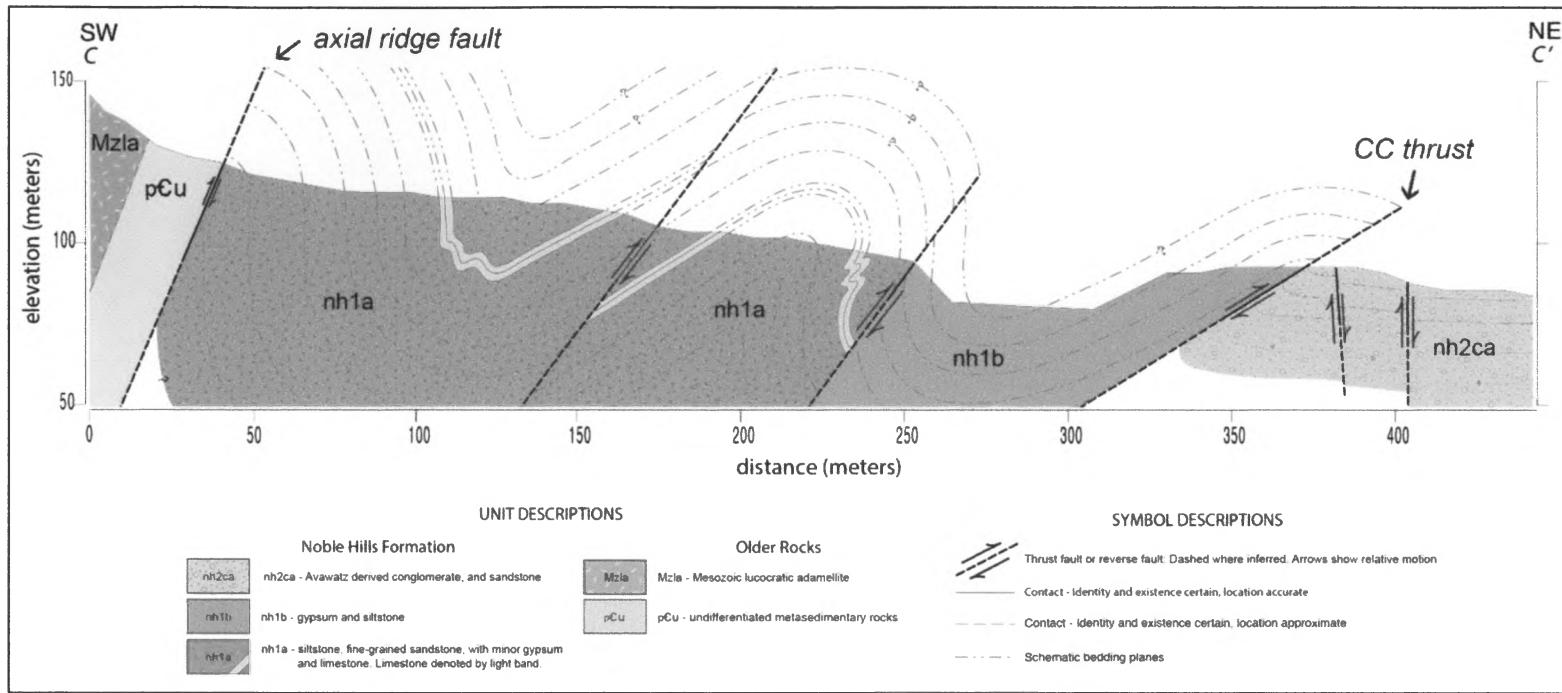


Figure 19: Cross section C-C' showing illustrating structural relations in the CC Wash area (Figure 6) in the area between the Axial Ridge fault and the vicinity of the CC thrust (Figure 20). See Plate 1 for cross section location.

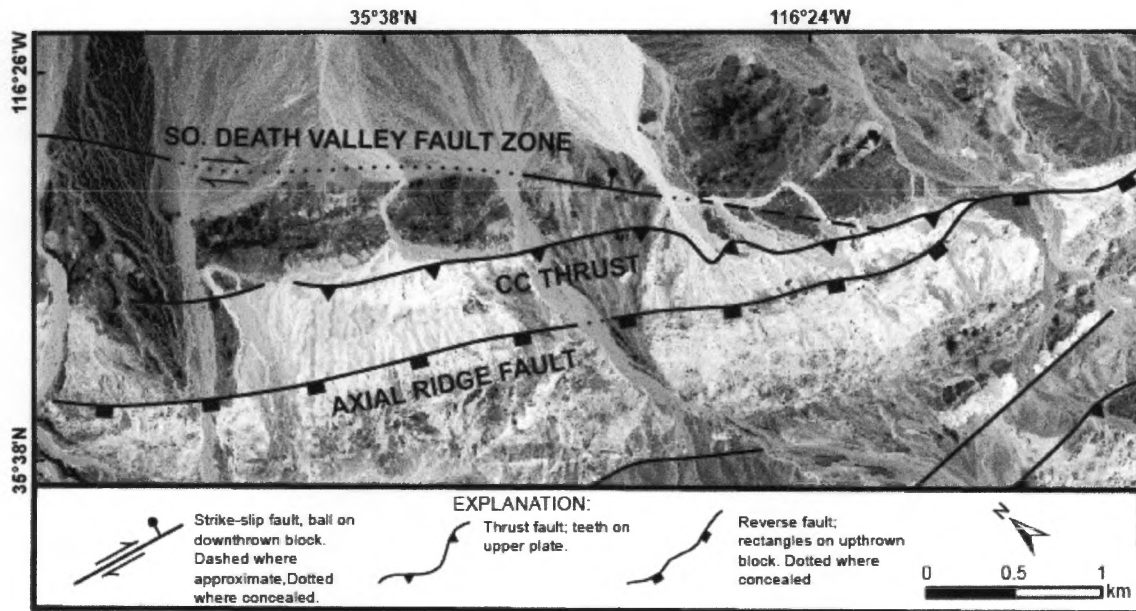


Figure 20: Generalized fault map showing the location of the three principle faults in the southern Noble Hills. From northeast to southwest, these faults are: the southern Death Valley fault zone (SDVFZ), CC thrust, and axial ridge fault (ARF).



Figure 21: Exposure of CC thrust in the Canadian Club Wash area (Figure 6). Gypsum of nh1b is thrust over halitic silts of nh1c. Teeth on thick dashed line are on upper plate. Depositional contact between the conglomerates and fines of nh2ca and halitic silts of nh1c can be seen on the left (thin dashed white line shows approximate contact). Geologist for scale.



Figure 22. View southeast of the Axial Ridge fault (thick dashed line) between Canadian Club and Amphitheater washes (Figure 6), showing Precambrian metasedimentary and Mesozoic granitic rocks (pCu + Mzla) thrust over complexly deformed strata of the Noble Hills Formation.

## 5.2 North-Striking Right Lateral Faults

Numerous north-striking right lateral faults were observed along the length of the Noble Hills. While only three of the faults were of moderate enough displacements to be mappable at the scale of Plate 1, unmappable, small-scale north-striking faults are abundant throughout the Noble Hills. Everywhere observed, these faults cross-cut northeast-vergent folds in the NHF. Based on measurement obtained from offset stratigraphic contacts of NHF strata measured both in the field and from geologic mapping (Plate 1), net offset of strata is approximately 80 m on faults in the Round Mountain area (Figure 6, Plate 1) and approximately 300 m in the Niter Field area

(Figure 6, Plate 1). These north-striking faults in the Niter Field project across the eastern trace of the SDVFZ but do not appear to offset it. Additionally, these faults are not expressed in capping conglomerate (Tf3) or Quaternary alluvial units (Qa1). Based on these observations, it is likely that movement on these faults preceded deposition of the Tf3 strata as well as movement on the eastern strand of the SDVFZ in the northern Noble Hills.

### **5.3 Southern Death Valley Fault Zone in the Vicinity of the Noble Hills**

Along the entire length of the Noble Hills, the SDVFZ is expressed as a mostly continuous, northwest-striking trace displacing Pliocene-to-Quaternary units (Plate 1). The following sections will describe the surface expression of the SDVFZ along the length of the Noble Hills, and subsequent use stratigraphic and structural relations to estimate the amount and timing of movement on the fault.

#### ***5.3.1 Surface Traces of the SDVFZ in the Noble Hills***

Surface expression of the SDVFZ is observable in the southern Noble Hills at two locations. At the north end of this section between Denning Spring and Cave Spring Washes (Figure 6: Index map of the Noble Hills) presumably late Pleistocene surface ruptures along the SDVFZ are somewhat weakly expressed as a left-stepping en echelon set of tonal lineaments in Qa2 alluvium (Figure 23). No discernable vertical or lateral displacements were observed along this trace.

At the mouth of CC Wash the SDVFZ is expressed as a large northeast-facing scarp in Qa1 alluvium that thinly mantles underlying members of the NHF (Figure 24). Although Qa1 surface shows an estimated 5 m of down-to-the-northeast vertical separation, the depositional contact between Qa1 and underlying megabreccia deposits locally exhibits a down to the southwest sense of vertical separation across the fault in this same area. These apparent contradicting relations are likely indicative of the predominantly lateral component of slip on the fault. At the mouth of CC Wash the SDVFZ cuts Qa2 deposits and underlying blocks of the nh2mb megabreccia (Figure 24). The expression of this strand shows approximately 5m of down-on-the-northeast separation, with no discernable right-lateral component in channels. This strand continues to the southeast where it loses clear expression. Previous workers have interpreted this strand as either continuing to the southeast as the contact between nh2c and nh2mb (Brady, 1986a), or as a discontinuous, down-on-the-northeast fault (Troxel and Brady, 1979; Stamm, 1981) only affecting the Qa2 deposit.

In the Niter Field area of the northern Noble Hills (Figure 6), the SDVFZ is expressed as a northeast-facing scarp in Qya1 alluvium (Plate 1). Here the SDVFZ is north-northwest striking and is interpreted as a continuation of the SDVFZ that is involved in transpressional deformation to the north of the Noble Hills, and on which a slip rate of ~0.2 to 0.4 mm/yr has been documented (Green, 2009; Plate 1). Surface expression of this ~6 km strand has been well documented along the northeast side of the Noble Hills by Green (2009), who reported numerous tectonic-geomorphic features

showing right-lateral, down-to-the-northeast displacement exclusively in Quaternary deposits.

A northwest-striking vertical fault is expressed in Qyal deposits to the west of the SDVFZ in the Niter Field area (Figure 6; Plate 1). A moderately degraded, up-to-the-NE scarp with ~0.5 m of vertical separation is present in alluvium immediately east of the nh1c beds in the Niter Field area with no discernable right-lateral offset (Figure 26). Continuation of this fault to the northwest of the Niter Field and into the Round Mountain area is unclear. Continuing to the southeast of the Niter Field area, the fault splays into at least two strands, one of which cuts obliquely to the nh1a member of NHF strata on the southwest side of the fault (Plate 1). Based on this observation, along with the structural interpretation for previous fault propagation folding, this western strand is interpreted to be a right-normal-oblique fault that formed after northeast-vergent fault-propagation folding of the NHF. Down-on-the-southwest motion along this strand is interpreted to have dropped backlimb nh1a strata in juxtaposition with halitic silts of nh1c across the fault (Figure 25). Based on its discontinuous nature, this fault is not interpreted to be a strand of the SDVFZ.

Structural relations presented here demonstrate that the Noble Hills section of the SDVFZ is a single strand that can be traced along the northeast side of the Noble Hills for most of its length, and cuts obliquely across depositional contacts within the previously deformed Pliocene stratigraphy of the NHF in the southern Noble Hills. This observation brings into question the existence of at least three previously mapped, major strands of

the SDVFZ of Brady (1984, 1986a) (Figure 4). Stratigraphic relations discussed in Section 4.1 show that two of these strands as mapped by Brady (1984, 1986a) are in fact steeply-tilted lithologic contacts within the conformable NHF. The interpretation by Brady (1984, 1986a) and Troxel (1994) that the Owlshead-Mountain-derived conglomerate (nh3, this study) is bounded on the southwest by a major strand of the SDVFZ is not supported by the observation that the unit nh3 is in conformable depositional contact with the underlying nh2f strata (Figure 7 & 15; Plate 1). Further, a fault juxtaposing these units would be required a consistent northeast facing dip of  $\sim 50^\circ$ - $70^\circ$  along most the contact. Similarly, the previously mapped major strand of the SDVFZ as mapped by Brady (1984, 1986a, 1986b) separating the halitic mudstone member (nh1c) and the megabreccia member (nh2mb) in the Salt Basin area (Figure 6; Plate 1) is in fact a high angle depositional contact (Figure 11D, Plate 1). Another previously mapped major trace of the SDVFZ by Brady (1984, 1986a, 1986b) juxtaposes nh1a (*Eastern Belt* of Brady, 1984; Figure 4) and Tf3 (*Older Quaternary fan deposits* of Brady, 1984; Figure 4) deposits in the northern Noble Hills; however, this contact was observed along its length as being an angular unconformity between the two units. Finally, the contact between the ARF and nh1a, as discussed in Section 5.1, appears to be a primarily a contractional feature in the southernmost Noble Hills, and transitions to the northwest to a more ambiguous contact (i.e., fault vs. depositional). These observations complicate the interpretation of this contact being a major strand of the right-lateral SDVFZ by Troxel and Butler (1979), Stamm (1981), and Brady (1984, 1986a, 1986b).

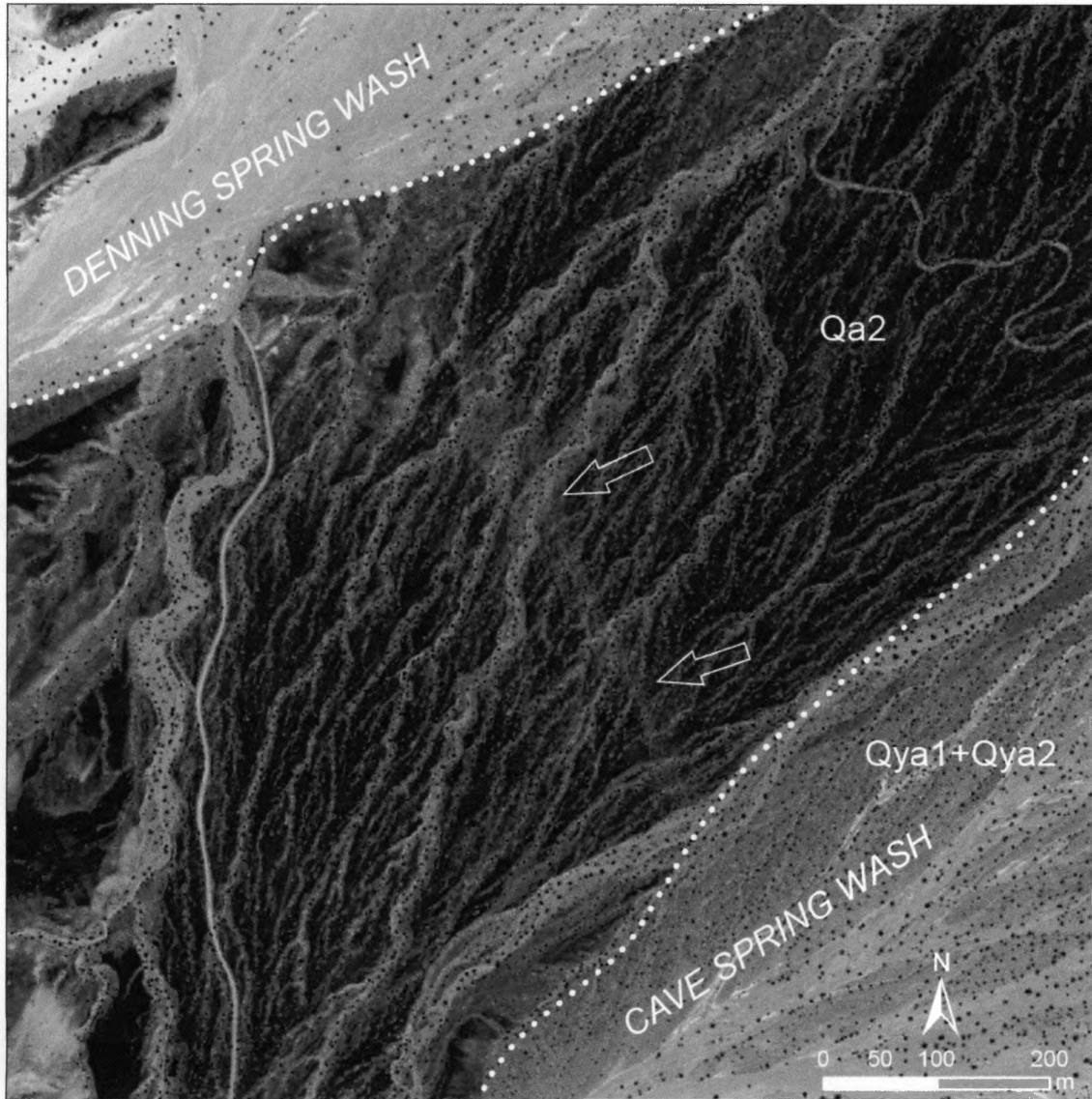


Figure 23: SDVFZ trace expressed as a subtle, left-stepping, en echelon tonal lineaments in Qa2 alluvium as indicated by arrows. Dotted white line indicates unit boundary. Note lack of offset channels in Qa2 and lack of expression in younger Qya1. No vertical displacement on this strand was observed. See Figure 20 for location.

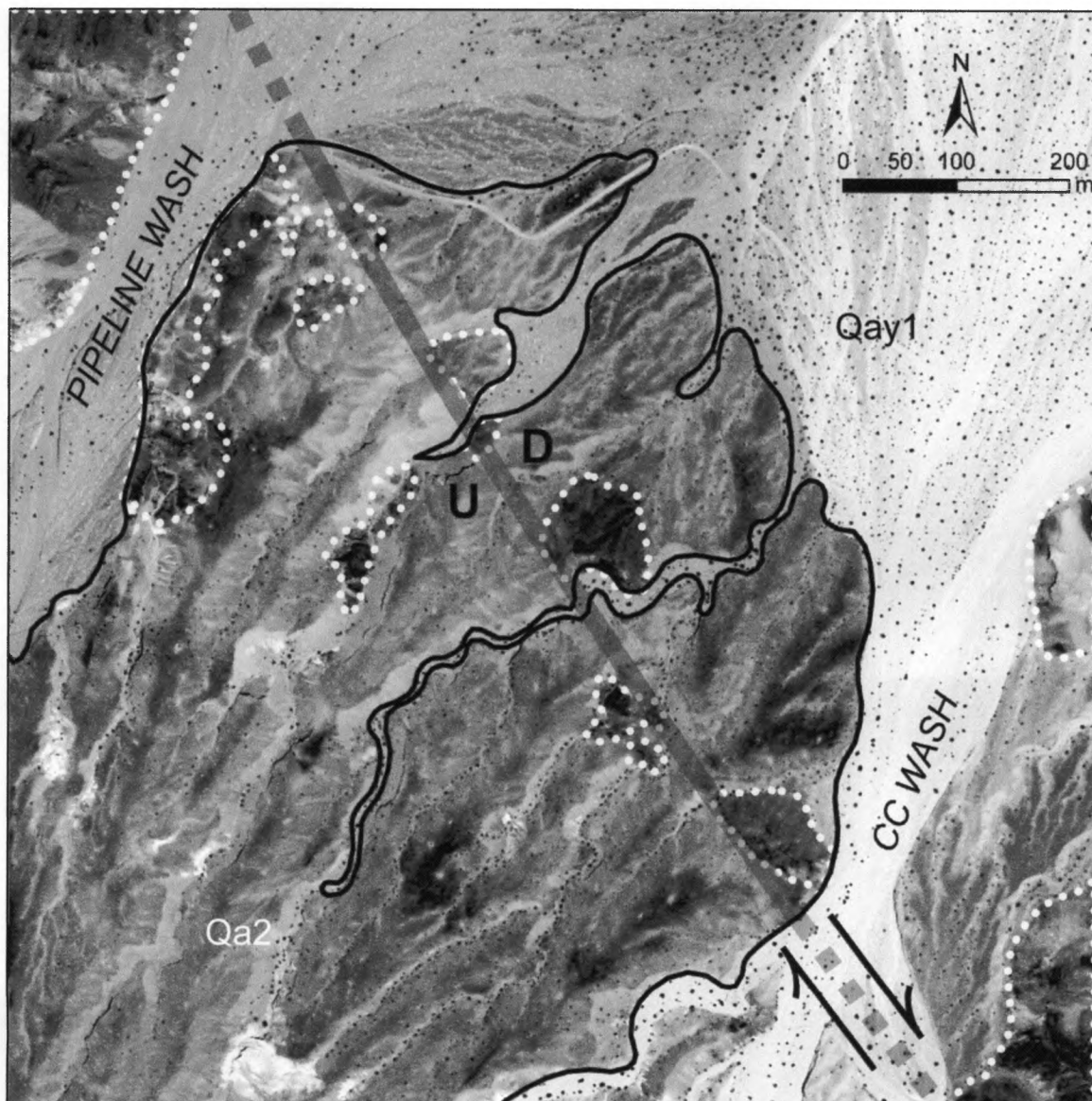


Figure 24: Trace of the SDVFZ in the CC Wash area: (gray line, dashed where concealed). White dotted lines denote megabreccia blocks (nh2mb) surrounded by Qa2 alluvium. Fault is down-on-the-northeast with no discernable channel deflection. See Figure 20 for location.

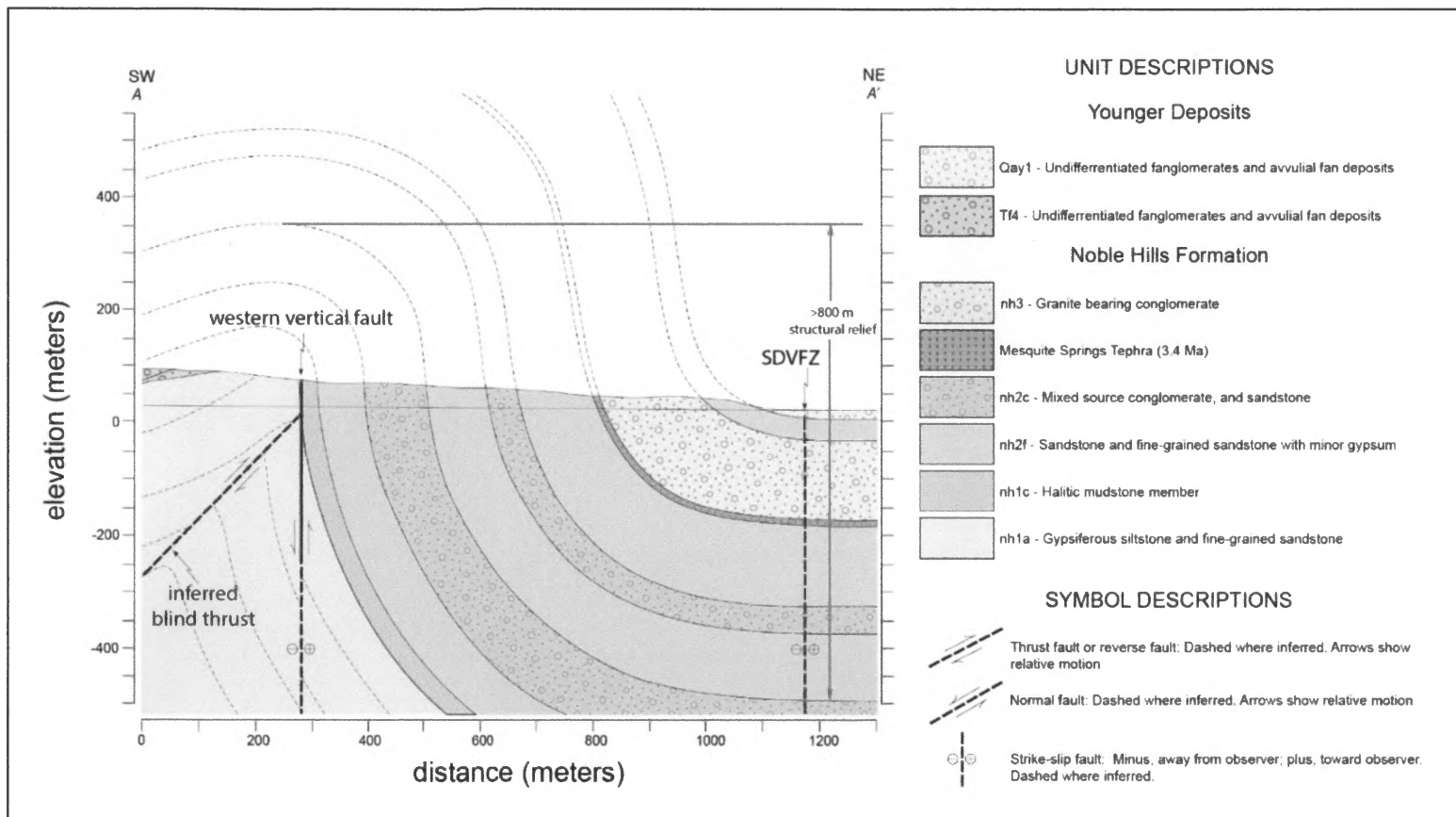


Figure 25: Cross section through the Niter Field area showing folding and faulting involving all members of the Noble Hills Formation, location of the SDVFZ (right), western vertical fault (left), and inferred blind thrust at depth.

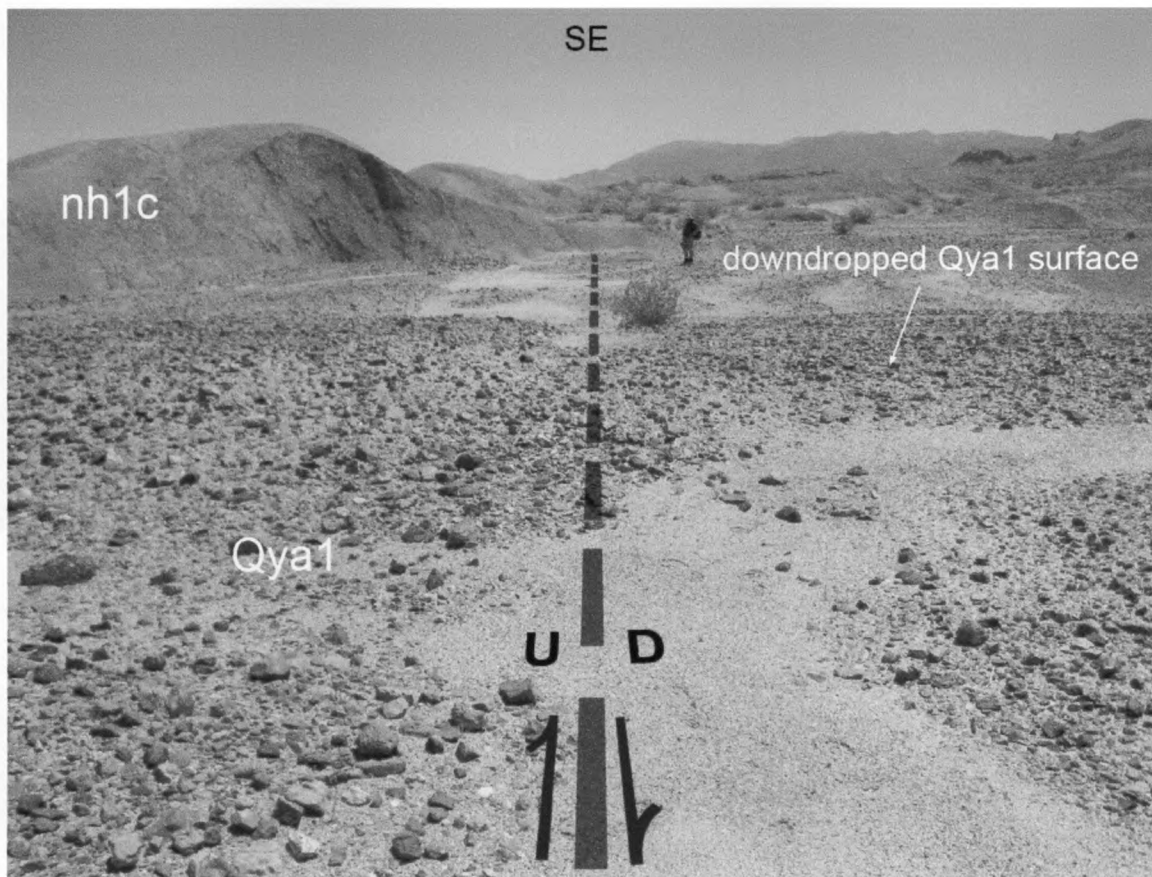


Figure 26: Tectonic geomorphic expression of high-angle fault in the Niter Field area of the northern Noble Hills. View is to the southeast. Dashed line shows approximate trace of the fault scarp. Movement is down-on-the southwest. No horizontal offset was discernable at this location.

### ***5.3.2 Constraints on post-middle Pliocene Offset along the SDVFZ***

Constraint on net right-lateral on the southern Noble Hills section of the SDVFZ is observed where the fault projects across a depositional contact in the Canadian Club Wash area. The projection of this fault trace to the southwest of the faulted Qa2 deposits (Figure 24) cuts oblique to the previously steeply-tilted depositional contact between the megabreccia of nh3 and the conglomerates of nh2c (Figure 27). While the nh3/nh2c contact is largely concealed beneath Qoa deposits on the southwest side of the fault, is exposed in several of the deep channel incisions, and the contact can be traced with confidence along its strike to that of the projected strike of the SDVFZ within an estimated uncertainty of a few tens of meters. On the northeast side of the fault, the trace of the nh3/nh2 contact is well exposed where it is truncated along the SDVFZ trace. Projected into the fault on either side of the SDVFZ trace, the nh3/nh2c contacts serve as piercing lines (A and A', Figure 27). Restoration of movement on this fault in excess of approximately 200 m is problematic as it would juxtapose incompatible stratigraphy across the fault. However, the geometry of the piercing line and the low angle of incidence in which the SDVFZ crosses it need not require any movement to attain the current configuration. Using the maximum offset of these deposits, which are stratigraphically correlated to the 3.34 Ma Mesquite Springs tephra bearing strata in the Niter Field area (Figure 7), a maximum slip-rate of ~0.06 mm/yr is possible but not required on this trace of the SDVFZ.

Where the SDVFZ is expressed as a tonal lineament in Qa2 alluvium at the mouth of Pipeline Wash (Figure 16), offset markers are absent, requiring that any significant right-lateral slip must occur prior to development of the Qa2 surface. Given the lack of offset markers on this trace, no slip-rate can be calculated.

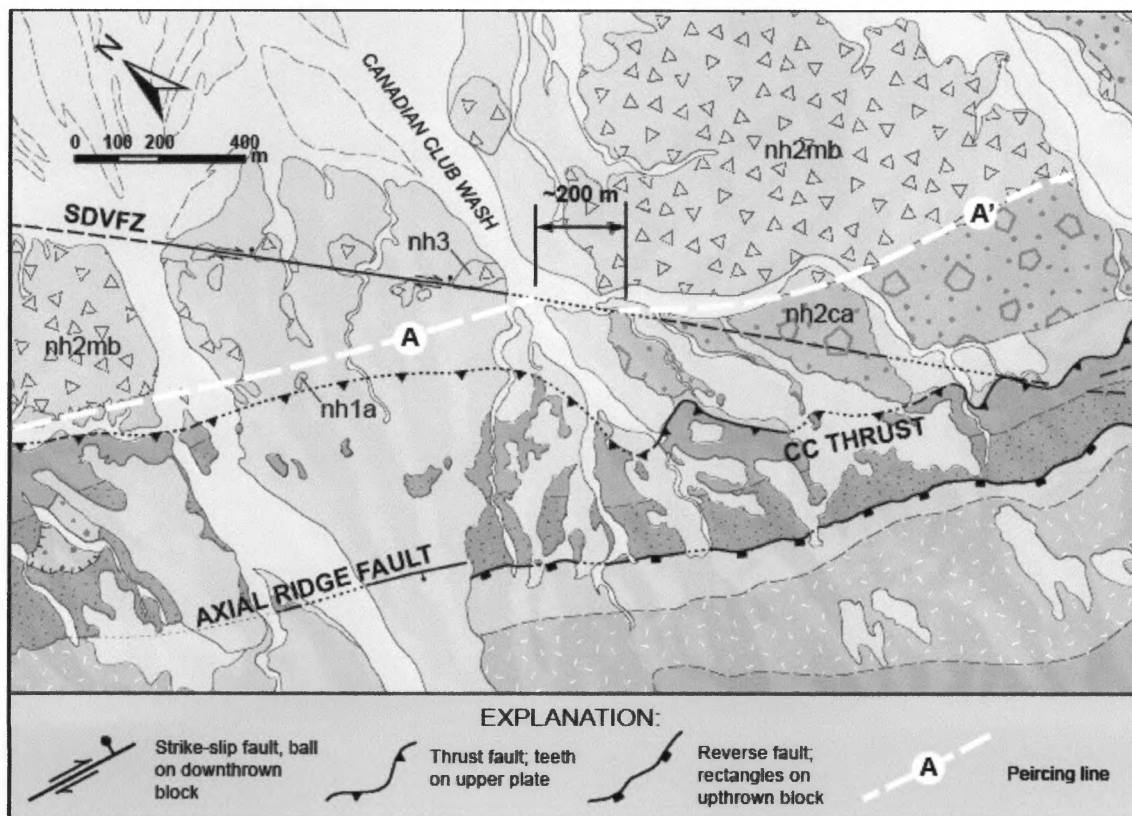


Figure 27: Geologic map of the Canadian Club Wash area (see Figure 6 for location) showing trace of the right-lateral-oblique-normal SDVFZ cutting Qa2 alluvium and projecting to the southeast across the piercing line created by the contact between nh2mb megabreccia and nh3 conglomerate at a shallow, oblique angle. Maximum offset based on this relationship is approximately 200 m. Note that orientation of piercing line does not require any restoration for current configuration.

Surface expression on the eastern strand of the SDVFZ in the northern Noble Hills displays down-on-the-northeast movement expressed in Quaternary deposits. No offset markers were documented in this study. Tectonic geomorphology along this strand was documented in detail by Green (2009), who noted right-lateral deflections of ~1.2 m in alluvial fan deposits estimated to be ~6-3 Ka in age, yielding a Quaternary slip-rate of 0.2 to 0.4 mm/yr.

The vertical fault to the west of the SDVFZ in the Niter Field area (Figure 28) does not display strike-slip offset markers.

The estimate of 8 km and 28 km of right-lateral offset along previously mapped strands of the SDVFZ in the Noble Hills as interpreted by Brady (1986a, 1986b) and Troxel (1994), respectively, relied on the restoration of conglomeratic strata in the Noble Hills to positions more proximal to the Owlshead Mountains to the northwest. Interpretation of the “granite-bearing conglomerate” of Brady (1986a, 1986b) and the fan gravel deposits of Troxel (1994) as being a tectonically-emplaced unit is not supported by the results of this study, which interprets these deposits (nh3, Section 4.1.7) as a conformable member of the NHF. Stratigraphic relations within the NHF complicate the interpretation of tectonic transport, as the nh3 member is interbedded and stratigraphically correlative with Avawatz Mountains-derived conglomerate of the nh2ca member (Figure 7). Further, any restoration of right-lateral movement on previously mapped strands would require that the conglomerate of nh2ca be moved further away from its source area to the south, and would equally affect the nh2mb megabreccia

deposits that were deposited proximal to the Avawatz Mountains, with are interpreted here as being conformable with the granite-bearing nh3 member.

Based on the evidence presented in this study for northeast-vergent contractional deformation of the conformable NHF, movement on the SDVFZ did not initiate on the Noble Hills segment of the SDVFZ until after 3.34 Ma, the correlated age of the Mesquite Springs tephra deposited within the uppermost NHF strata. Where the SDVFZ is observable north of the Noble Hills, Green (2009) interpreted that segment as a persistent left-step affecting middle Pliocene strata. Initiation of movement on the Confidence Hills segment of the SDVFZ was shown by Goodman (2010) to have not begun until after  $\sim 0.9$  Ma, yielding a slip rate of  $\sim 0.7$  mm/yr. Constraining initiation of slip on the step-over and Noble Hills segments of the SDVFZ to that obtained on the Confidence Hills segment by Goodman (2010), yields post-middle-Pleistocene right-lateral slip rates of  $\sim 0.5$  mm/yr and  $\sim 0.2$  mm/yr, respectively. These slip rates for the SDVFZ are in marked contrast to those obtained on the NDVFZ (Table 1), and present complications for the Death Valley pull-apart model of Burchfiel and Stewart (1966).

### ***5.3.3 Constraints on longer-term offsets on the SDVFZ***

The interpretation by Brady (1984) and Brady and Troxel (1999) of 20-23 km of right-lateral offset along an inferred southward continuation of the SDVFZ based on the displacement Military Canyon Formation from its presumed source is problematic based on lithologic correlations between the southern Salt Spring Hills and the Avawatz Mountains (Figure 3). Mapping in the southern Salt Spring Hills by Troxel (1967) reveals

a kilometer-thick section of late Precambrian to Cambrian rocks intruded by Mesozoic(?) quartz monzonite (Figure 28). Mapping by Spencer (1990a, 1990b) documents extensive exposures of intrusive rocks that make pre-Cenozoic basement of the Avawatz Mountains termed the Avawatz quartz monzodiorite complex. Spencer (1990a) described this intrusive complex as being variable in composition, ranging from diorite to quartz monzodiorite, granodiorite, granite, and quartz monzonite. Spencer (1990b) maps an intrusive contact between the Avawatz Quartz monzodiorite complex and Precambrian Johnnie Formation within the Avawatz Mountains approximately 10 km south-southwest of the southern Salt Spring Hills (Figure 29).

During reconnaissance for this study, field observations made of both the southern Salt Spring Hills quartz monzonite and the intrusive rocks of the Avawatz Quartz Monzodiorite complex of Spencer (1981, 1990a) found in the hanging wall of the Old Mormon Spring fault revealed remarkably similar composition in hand sample. The correlation of these two intrusive bodies, while speculative, would complicate previous estimates of large-magnitude offset on any previously mapped strand of the SDVFZ, as the Noble Hills section of the SDVFZ is terminated by the Mule Springs fault in the northeastern Avawatz Mountains (Davis, 1977; Troxel and Butler, 1998); similarly, Spencer (1990) suggests that, if it did exist, the inferred southern extension of the SDVFZ would be truncated by the Old Mormon Springs fault in the eastern Avawatz Mountains. This places a throughgoing SDVFZ in a position between the southern Salt Spring Hills and the Avawatz Mountains following deposition of the Military Canyon Formation and

preceding termination by the Mule Springs and Old Mormon Springs faults. Based on the similar intrusive relationship between Precambrian Johnnie Formation and lithologically similar plutonic rocks exposed in the Avawatz Mountains and southern Salt Spring Hills (Figure 29), which are juxtaposed across the inferred trace of the SDVFZ, restoration of large-magnitude right-lateral displacement on this trace to account for the source material for the Military Canyon Formation becomes problematic.

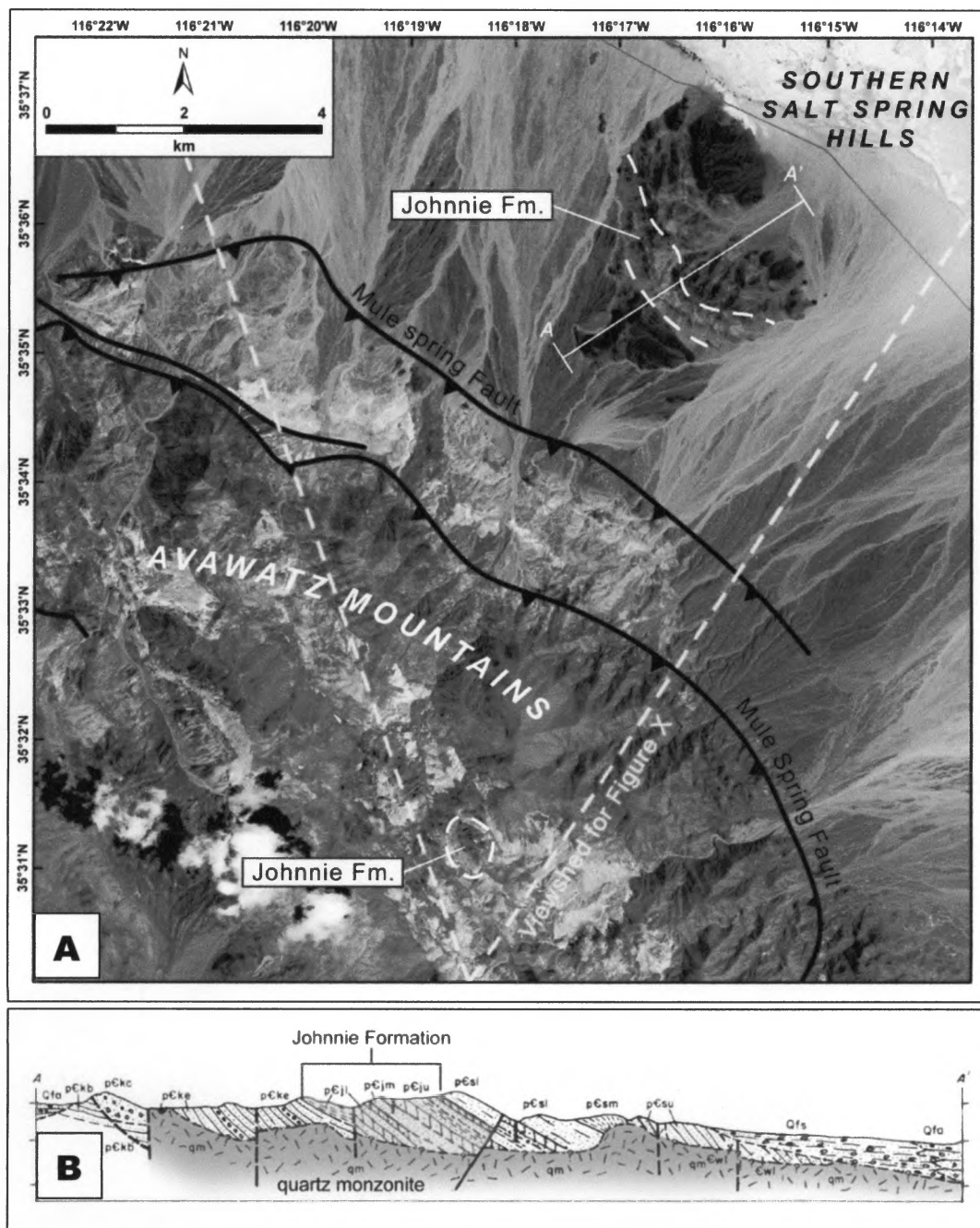


Figure 28: A) Map of the northeast Avawatz Mountains and Southern Salt Spring Hills showing location of Johnnie Formation, cross section line, and viewshed of Figure 30. Mapping modified from Troxel (1967) and Spencer (1981). B) Cross section of the Southern Salt Spring Hills showing intrusive contact between Mesozoic(?) quartz monzonite and Precambrian strata, notably the Jonnie Formation (Troxel, 1967)

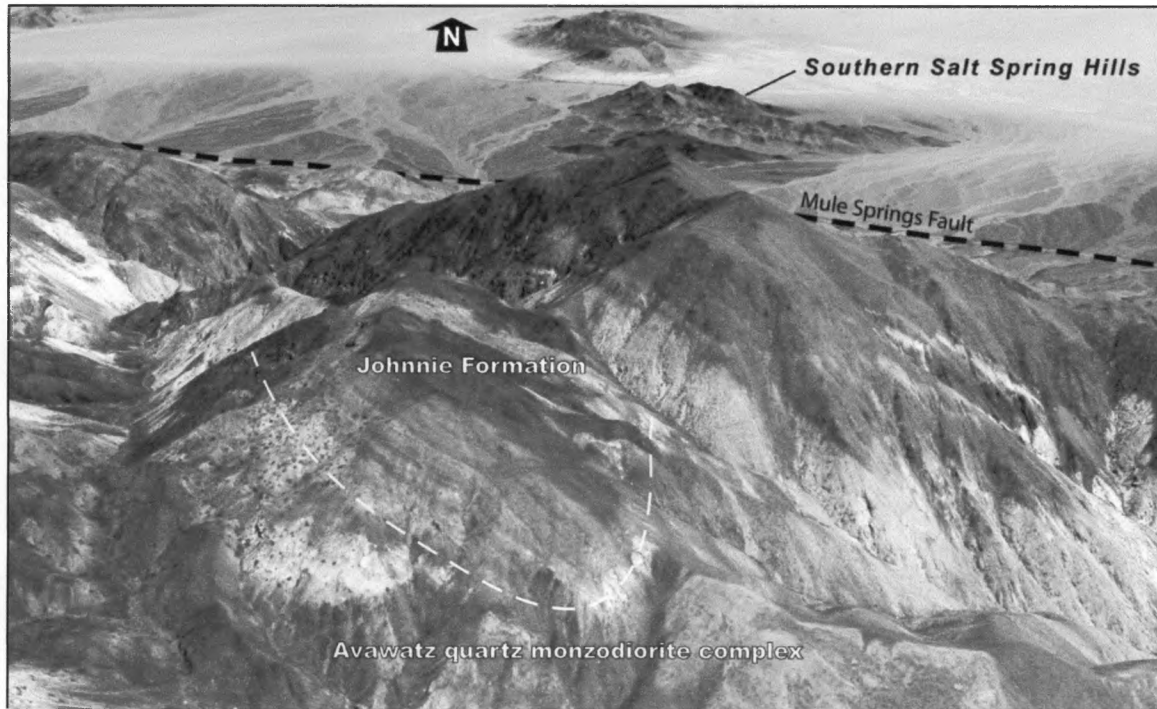


Figure 29: Oblique view of the Avawatz Mountains (foreground) and the Southern Salt Spring Hills showing intrusive contact between the Johnnie Formation and the Avawatz Mountains quartz monzodiorite complex of Spencer (1990b). See Figure 29A for viewshed location. Imagery from Google Earth, 2014.

## **6.0 SUMMARY AND DISCUSSION**

The following *Summary and Discussion* section is subdivided into two subsections. The first will summarize the interpretations of depositional environments of the Noble Hills Formation presented in Section 4.0 as a framework for building a basin history and interpreting the paleogeography of the basin. The second section will discuss the kinematic models for deformation in the Noble Hills in the context of northeast Mojave block transrotation.

### **6.1 Summary and Interpretation of the Noble Hills Formation**

The strata of the Noble Hills Formation form a nearly intact basin sequence that records the history of sedimentation in the Pliocene Noble Hills basin. These changes reflect both changes in depositional environment and source areas for clastic strata.

The oldest exposed strata of the NHF were deposited in an ephemeral lacustrine setting as recorded by the nh1a member of the NHF. The depositional surface on which the basin formed is unclear. However, given the observation of a depositional contact between the sandstones and pebble-conglomerate of nh1a and the rocks of the axial ridge, as well as the high percentage of angular felsic clasts in the pebble-conglomerate facies, it is not unreasonable to assume that the rocks that now form the axial ridge served as both the original depositional surface and as a sediment source. Upsection of the nh1a member, the NHF fines to include gypsiferous siltstones and halitic mudstones that were formed in a mix of ephemeral lacustrine, saline mudflat and saline lake depositional environments. This fining upwards may reflect an overall lowering of the basin

coincident with regional extension and normal faulting on the Avawatz Mountains range front. The next stage in the history of the basin involved the progradation of alluvial fans into a lacustrine and playa environment, which is recorded in deposition of the mixed lithology sediments of nh2ca and nh2c. In the southern Noble Hills, nh2ca conglomerates consist of clasts derived exclusively from the proximal Avawatz Mountains, while nh2c conglomerate in the north suggest the integration of fans emanating from the Owlshead Mountains and areas west of the Avawatz Mountains. Additionally, the nh2c deposits record several intervals of fine-grained strata (nh2f) that represent either climatic fluctuations or changes in fan extent. In the southern Noble Hills, catastrophic emplacement of the landslide blocks onto the alluvial fan and saline mudflat environments effectively stopped deposition into this part of the basin. To the north, lacustrine and playa environments persisted and the silts and gypsums of nh2f enveloped the landslide mass of nh2mb at its furthest northern extent in the Denning Spring area (Figure 6, Plate 1). The stratigraphically youngest exposed member of the NHF records the input of predominantly Owlshead Mountains derived lithologies of the nh3 conglomerate. In the Niter Field area (Figure 6), deposition of the marginal lacustrine fine-grained deposits of nh2f and the fluvial granitic-rich conglomerate, nh3, is temporally constrained to 3.34 Ma by the presence of the Mesquite Springs tephra.

The results of this study strongly suggest that the NHF is a conformable stratigraphic sequence that is constrained to be post-Middle Pliocene and older in age. Given this interpretation, previous interpretations that require tectonic emplacement of

the granitic conglomerate along strands of a strike-slip fault zone (Brady 1986a, 1986; Troxel, 1994) is not supported.

## **6.2 Transrotation of the Northeast Mojave Block and Tectonic Development of Southern Death Valley**

New observations that offsets along the SDVFZ in the Noble Hills are on the order of only hundreds of meters and that the movement on the fault clearly began after intensive shortening of the Pliocene NHF indicate that transpressional shearing along the SDVFZ is no longer a valid mechanism for the northeast vergent contraction in the Noble Hills. It is proposed here that clockwise transrotation of the northeast Mojave block (Garfunkel, 1974; Carter et al., 1984; Schermer et al., 1996), and concomitant north-directed compression from the northern boundary of the block, provided the driving mechanism in for post-3.4 Ma and post 1.0 Ma northeast-vergent deformation in the Noble Hills and Confidence Hills, respectively (Goodman, 2010; Caskey et al., 2010). Earlier northeast-vergent contraction in the Confidence Hills, as in the Noble Hills, is well constrained to predate movement on the SDVFZ (Goodman, 2010). Contractional deformation of the Confidence Hills Formation (Beratan, et al., 1999) terminates to the north precisely at the along-strike projection of the north-east striking, left-lateral, Wingate Wash fault (Figure 30). North of this point, the style of strain along the Death Valley fault system abruptly changes to transtensional (Serpa and Pavlis, 1996). In the central part of the Confidence Hills, northeast-striking left-lateral faults strike perpendicular to and disrupt overturned, northeast-vergent folding south of Confusion

Canyon where folds show left-lateral bending at the along-strike projection of the same zone of left-lateral faults.

The more recent detailed field investigations in the Noble Hills (this report) and Confidence Hills (Goodman, 2010) reveal remarkably similar tectonic histories for the northern and southern parts of SDV and similar conclusions regarding evidence for small net offsets on the SDVFZ and a much more recent first appearance in SDV than ever suggested by earlier field investigators.

The kinematics for earlier intensive contraction appears to be relatively straightforward. As the northern boundary of the northeast Mojave block has rotated clockwise toward the Owlshead Mountains, resultant north-directed compression has impinged upon the Owlshead Mountains (Figure 30). Preexisting northeast-striking left-lateral faults such as the Wingate Wash fault, northeast-striking faults in the central Owlshead Mountains, perhaps the Owl Lake fault, and a fault that is inferred along the southeastern margin of the Owlsheads that would project northeast to north end of the northern Noble Hills, where earlier northeast-vergent folding appears to end.

The conspicuous north-striking right-lateral faults that cross-cut the northeast-vergent folds and thrusts in the Nobel Hills and appear to predate the northwest-striking trace of the SDVFZ likely owe their origin to a late stage of transrotation of the northeast Mojave block (Figure 29, 30 & 31). Important to this notion is that the axis of clockwise rotation of the northeastern Mojave block appears to lie in the east-central part of the Avawatz Mountains. This follows because northeast-directed contractional faulting along

the east side of the Avawatz Mountains, which is generally accepted to be a consequence of block rotation, ends abruptly where the Mormon Springs fault bends southeastward just south of Mormon Springs Canyon. This is a similar conclusion reached by Guest et al (2003). In this structural setting the north-striking faults develop because the areas immediately north of the rotating block boundary that are farther west of the axis of rotation get pushed (i.e., displaced) farther north than areas closer to the rotation axis. This kinematic setting therefore favors the development of north-striking right-lateral shears to accommodate differential northward displacement.

The Schermer et al. (1996) paleomagnetic data and model for the northeast Mojave block suggests that greater than 30 km of distributed right-lateral shear has been transferred northward by vertical axis rotation since 10 Ma (Figure 31). Yet the results of new and recent investigations in the Confidence Hills (Goodman, 2010) and the Noble Hills would suggest that very little of that shear for at least the last few million years has been transferred through SDV.

Schermer et al. (1996) in support of their model cite estimates by Brady (1984b, 1994) and Troxel (1994) of 25 to 28 km of right-lateral offset on the SDVFZ. That fact that Schermer et al. are trying to accounting for the 30+ km of transrotation by discreet slip on faults that bound the east and west borders of the block indicate that they seem to be overlooking an important geometric aspect of the model, in that the 30+ km of transrotation can be accomplished with little to no discreet right-lateral slip on the east and west boundaries of the block. Furthermore, if the northeast Mojave block is pinned

on the northeast corner rather than the northwest corner, as they show, the northward transfer of distributed shear would be cumulative toward the west, the transfer of slip into southern Death Valley would be expected to be very small, which is what recent field investigations convincingly show. Questions remain regarding details of ECSZ kinematics, specifically how right-lateral shear is ultimately transferred into northern Death Valley to account for the high slip rate on the NDVFZ.

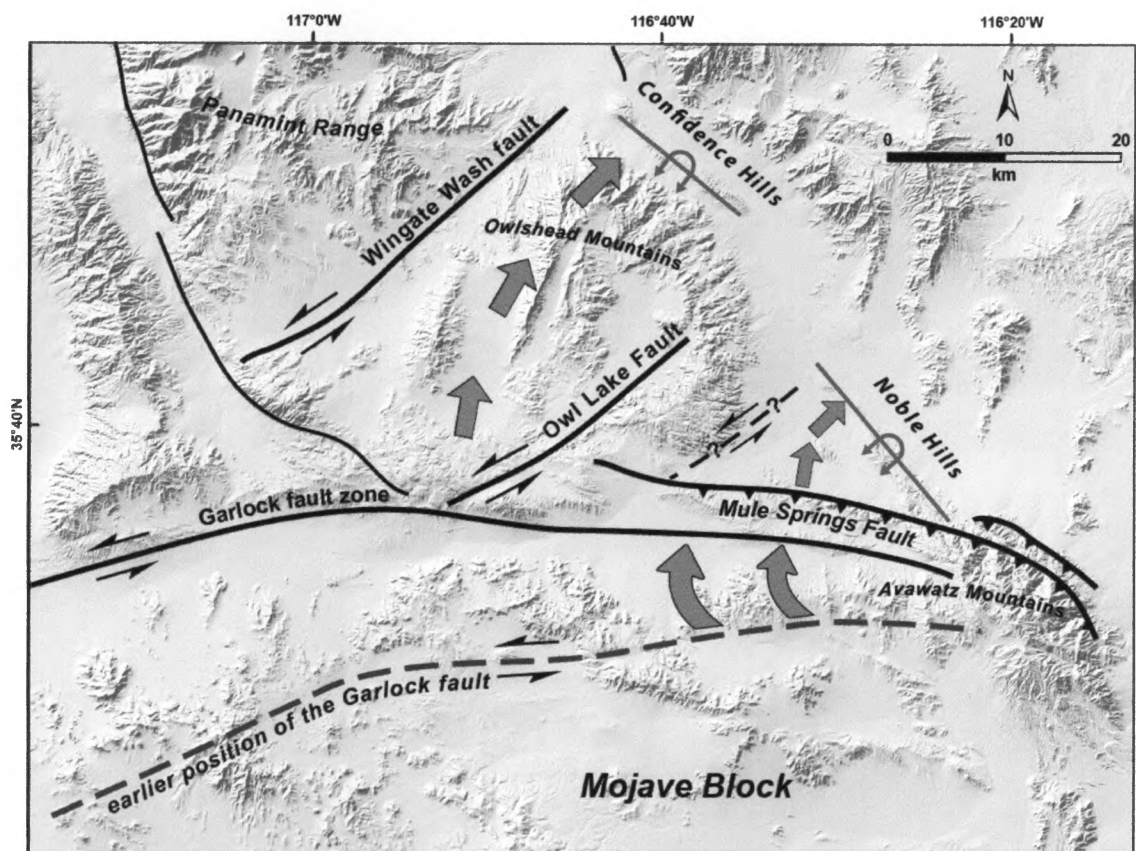


Figure 30: Model of progressive deformation of the Noble Hills and Confidence hills basin deposits as the result of clockwise rotation of the Mojave Block, and resulting impingement into the southern Death Valley region.

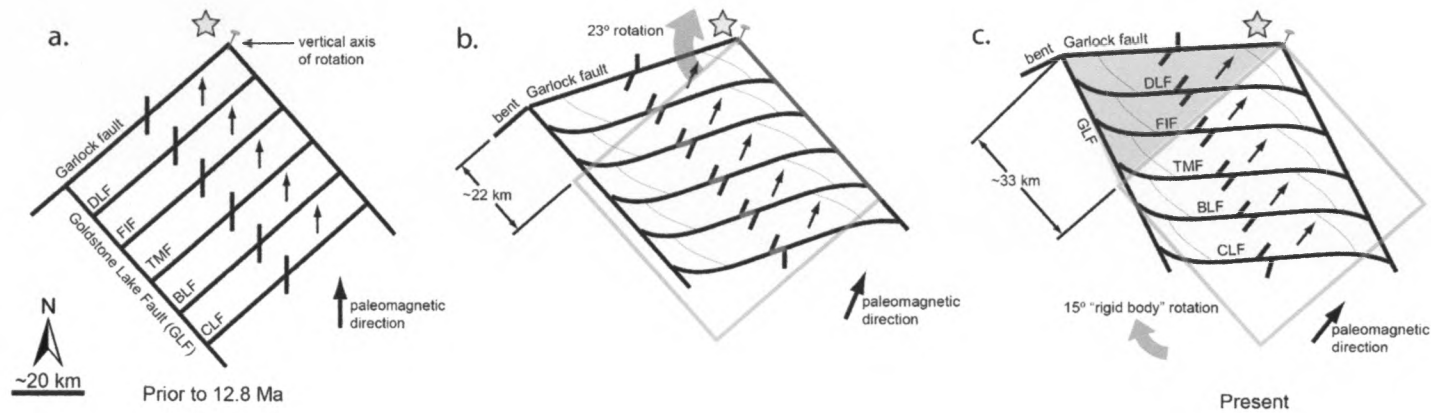


Figure 31: Cartoon block model illustrating rotational model of the northeast Mojave domain modified from Schermer et al. (1996). Model shows progressive deformation of faults within the northeast Mojave domain and the bounding Garlock fault. (a) Original orientation of the northeast Mojave domain, and paleomagnetic indicators. Axis of rotation is located around a point located approximately in the Avawatz Mountains (b) 5 km of left slip on faults within the domain (red lines) resulting in ~23 km of rotation, and bending of the Garlock fault. Grey square is reference frame. (c) 15° of "rigid body" rotation of the domain, and bent Garlock fault. Grey square is reference frame. The resulting dextral shear of ~33 km is inferred to be transferred to the domain north of the Garlock fault. Star denotes location of the Noble Hills basin.

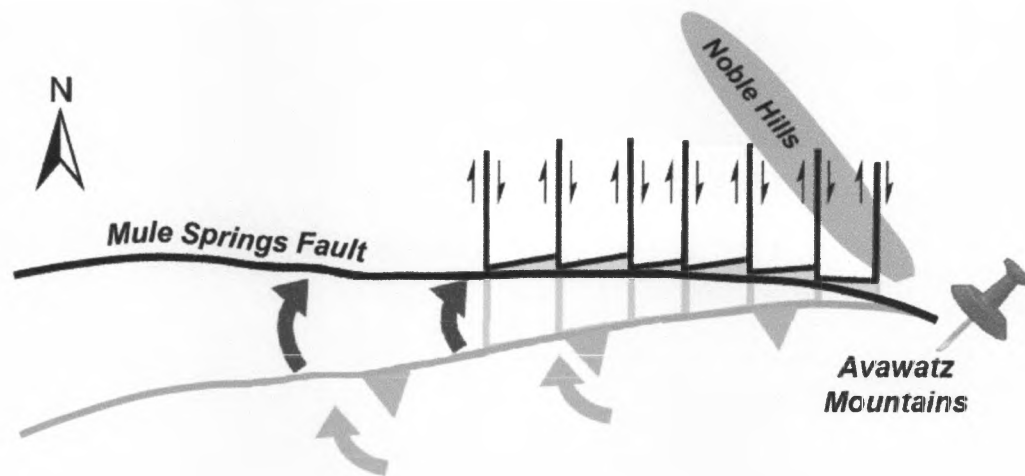


Figure 32: Model of mechanism for north-striking faulting in the Noble Hills being driven by clockwise rotation of the northeast Mojave block around a point in the Avawatz Mountains.

## 7.0 CONCLUSIONS

The tectonic development of the Noble Hills began with the deposition of an approximately 800 m thick sedimentary sequence of conformable, coarsening-upwards deposits (the NHF). These deposits received sedimentary input from the surrounding Avawatz and Owlshead Mountains by fluvial transport, as recorded by the mostly continuous, and conformable conglomeratic strata of nh2c and nh2ca. Tephra sampled from strata in the upper NHF constrains the age of the uppermost NHF to be 3.34 Ma. Clockwise rotation of the northeast Mojave domain about an axis located approximately within the Avawatz Mountains impinged on the Noble Hills basin, causing systematic northeast-vergent folding and faulting. The NHF records intensive northeast-vergent folding and thrusting in the southern Noble Hills, and large-scale, northeast-vergent fault-propagation folding in the northern Noble Hills, consistent with rotation about an axis south of the Noble Hills. Following contractional deformation, the NHF experienced extensive erosion, succeeded by deposition of numerous alluvial fan deposits sourced primarily from the Avawatz Mountains. The SDVFZ subsequently offset middle-early Pleistocene alluvial fan deposits and underlying NHF deposits a maximum of approximately 200 m.

**REFERENCES**

- Beratan, K. K., Hsieh, J., and Murray, B., 1999, Pliocene-Pleistocene stratigraphy and depositional environments, southern Confidence Hills, Death Valley, California: in Wright, L.A., and Troxel, B.W., eds., *Cenozoic Basins of the Death Valley Region*: Boulder, Colorado, Geological Society of America Special Paper 333, p. 289-299.
- Brady III, R.H., 1984, Neogene stratigraphy of the Avawatz Mountains between the Garlock and Death Valley fault zones, southern Death Valley, California: Implications as to late Cenozoic tectonism: *Sedimentary geology*, v. 38, no. 1-4, p. 127-157.
- Brady III, R.H., 1986a, Cenozoic geology of the northern Avawatz Mountains in relation to the intersection of the Garlock and Death Valley fault zones: San Bernardino County, California [Ph. D. thesis]: Davis, University of California, v. 292.
- Brady, R.H., 1986b, Stratigraphy and tectonics of the northern Avawatz Mountains at the intersection of the Garlock and Death Valley fault zones, San Bernardino County, California – A Field Guide in Troxel, B.W., ed., *Quaternary Tectonics of Southern Death Valley, California, Field Trip Guide, 1986*, Pacific Cell, Friends of the Pleistocene, 44 pp.
- Brady, R. H., 1994, The Miocene Military Canyon Formation: Depocenter destruction and constraints on lateral faulting, southern Death Valley, California, *Geol. Soc. Am. Abstr. Programs*, 26,41.
- Brady, R.H., and Troxel, B.W., 1999, The Miocene Military Canyon Formation: Depocenter evolution and constraints on lateral faulting, southern Death Valley, California: *Special Papers-Geological Society Of America*, p. 277-288.
- Burchfiel, B.C., and Stewart, J.H., 1966, "Pull-apart" origin of the central segment of Death Valley, California: *Geological Society of America Bulletin*, v. 77, no. 4, p. 439-442.
- Butler, P.R.A., Troxel, B.W., and Verosub, K.L., 1988, Late Cenozoic history and styles of deformation along the southern Death Valley fault zone, California: *Bulletin of the Geological Society of America*, v. 100, no. 3, p. 402.

- Caskey, S. J., Goodman, J. T., Green, H.L., Niles, J.H., Wan, E., Wahl, D.B., Olsen, H.A., 2010, Constraints on post-middle-Pleistocene offsets and new perspectives on Plio-Pleistocene tectonism along the Southern Death valley fault zone. Geological Society of America Abstracts with Programs, v. 42, n. 4, p. 55
- 2010, Constraints on post-middle-Pleistocene offsets and new perspectives on Plio-Pleistocene tectonism along the Southern Death valley fault zone. Geological Society of America Abstracts with Programs, v. 42, n. 4, p. 55
- Carter, J., Luyendyk, B. P., and Terres, R. R., 1987, Neogene clockwise tectonic rotation of the eastern Transverse Ranges, California, suggested by paleomagnetic vectors: Geological Society of America Bulletin, v. 98, p. 199-206.
- Durrell, C., 1953, Geological investigations of strontium deposits in southern California: California Div: Mines Spec. Rept, v. 32, p. 48.
- Davis, G.A., 1977, Limitations on displacement and southeastward extent of the Death Valley fault zone: California: Short contributions to California Geology: Special report: California Divisions of Mines and Geology, v. 129, p. 27–33.
- Dokka, R.K., and Travis, C.J., 1990, Late Cenozoic strike-slip faulting in the Mojave Desert, California: Tectonics, v. 9, no. 2, p. 311–340.
- Dooley, T. P., and McClay, K. R., 1996, Strike-slip deformation in the Confidence Hills, southern Death Valley fault zone, eastern California, USA: Journal of the Geological Society, v. 153, p. 375-387.
- Frankel, K. L., Dolan, J.F., Finkel, R.C., Owen, L.A., and Hoeft, J.S., 2007a, Spatial variations in slip rate along the Death Valley-Fish Lake Valley fault system 108 determined from LiDAR topographic data and cosmogenic  $^{10}\text{Be}$  geochronology: Geophysical Research Letters, v. 34, p. L18303.
- Frankel, K. L., Brantley, K.S., Dolan, J.F., Finkel, R.C., Klinger, R.E., Knott, J.R., Machette, M.N., Owen, L.A., Phillips, F.M., Slate, J.L., and Wernicke, B.P., 2007b, Cosmogenic  $^{10}\text{Be}$  and  $^{36}\text{Cl}$  geochronology of offset alluvial fans along the northern Death Valley fault zone: Implications for transient strain in the eastern California shear zone: Journal of Geophysical Research, v. 112, p. B06407.
- Garfunkel, Z., 1974, Model for the late Cenozoic tectonic history of the Mojave Desert, California, and for its relation to adjacent region, Geol. Soc. Am. Bull., 1931-1944, p. 85

- Goodman, J.T., 2010, Post-middle-Pleistocene Tectonic Development of the Confidence Hills, Death Valley, California: San Francisco State University.
- Green, H.L., 2009, Neotectonic Investigation of the Southern Death Valley Fault Zone, Southeastern California: San Francisco State University.
- Guest, B., Pavlis, T.L., Golding, H., and Serpa, L., 2003, Chasing the Garlock: A study of tectonic response to vertical axis rotation: *Geology*, v. 31, p. 553–556
- Hamilton, W., and Myers, W.B., 1966, Cenozoic tectonics of the western United States: *Reviews of Geophysics*, v. 4, no. 4, p. 509–549.
- Harding, T.P., 1985, Seismic characteristics and identification of negative flower structures, positive flower structures, and positive structural inversion: *AAPG Bulletin*, v. 69, no. 4, p. 582–600.
- Howard, J.L., 1993, The statistics of counting clasts in rudites: a review, with examples from the upper Palaeogene of southern California, USA: *Sedimentology*, v. 40, no. 2, p. 157–174.
- Jennings, C. W., Burnett, J.L., and Troxel, B.W., 1963, Geologic map of California, Trona Sheet: California Division of Mines and Geology, scale 1:250,000.
- Klinger, R. E., 1999, Tectonic geomorphology along the Death Valley Fault System - Evidence for recurrent late Quaternary activity in Death Valley National Park: United States Geological Survey, Open-File Report 99-153, p. 132-140.
- Klinger, 2001, Evidence for large dextral offset near Red Wall Canyon *in* Machette, M.N., Johnson, M.L., and Slate, J.L., eds., *Quaternary and Late Pliocene Geology of the Death Valley Region: Recent Observations on Tectonics, Stratigraphy, and Lake Cycles: Pacific Cell- Friends of the Pleistocene Field Trip*, p. A32-A37.
- Klinger, R., and A. Sarna-Wojcicki, 2001. Active tectonics and deposition in the Lake Rogers basin, USGS OFR 01-0051, p. 25–31.
- Klinger, R.E., 2002. Quaternary stratigraphy and geomorphology of northern Death Valley — Implications for tectonic activity along the northern Death Valley fault, Ph.D. thesis, University of Colorado, Boulder, 312 pp.
- Machette, M.N., Klinger, R.E., Knott, J.R., Wills, C.J., Bryant, W.A., and Reheis, M.C., 2001, A proposed nomenclature for the Death Valley fault system: *Quaternary and*

Late Pliocene Geology of the Death Valley Region: Recent Observations on Tectonics, Stratigraphy, and Lake Cycles (Guidebook for the 2001 Pacific Cell—Friends of the Pleistocene Fieldtrip), p. 173.

- Menges, C. M., and Miller, D. M., 2007, Introduction *in* Miller, D. M., Menges, C. M., and McMackin, M., eds., *Geomorphology and Tectonics at the Intersection of Silurian and Death Valleys: Pacific Cell Friends of the Pleistocene, 2005 Guidebook*: United States Geological Survey, Open-File Report 07-1424, p. 1-7.
- Miall, A.D., 1977. Lithofacies types and vertical profile models in braided river deposits: a summary. In: A.D. Miall (Editor), *Fluvial Sedimentology*. Can. Soc. Petrol. Geol. Mem., 5: 597-604
- Miller, M.M., Johnson, D.J., Dixon, T.H., and Dokka, R.K., 2001, Refined kinematics of the Eastern California shear zone from GPS observations, 1993-1998: *Journal of Geophysical Research*, v. 106, no. B2, p. 2245–2264.
- Noble, L.F., and Mansfield, G.R., 1922, Nitrate deposits in the Amargosa region, southeastern California: U.S. Geol Survey Bull. 724
- Noble, L.F., and Wright, L.A., 1954, *Geology of the central and southern Death Valley region, California*: Jahns.
- Ver Planck, W.E., 1952, *Gypsum in California*: State of California, Dept. of Natural Resources, Division of Mines.
- Schermer, E.R., Luyendyk, B.P., and Cisowski, S., 1996, Late Cenozoic structure and tectonics of the northern Mojave Desert: *Tectonics*, v. 15, no. 5, p. 905–932.
- Serpa, L., and Pavlis, T., 1996, Three-dimensional model for the late Cenozoic history of the Death Valley region, southeastern California: *Tectonics*, v. 15, p. 1113–1128
- Smith, G.I., 1962, Large Lateral Displacement on Garlock Fault, California, as Measured from Offset Dike Swarm: *AAPG Bulletin*, v. 46, no. 1, p. 85–104.
- Spencer, J.E., 1981, *Geology and geochronology of the Avawatz Mountains, San Bernardino County, California* [Ph.D. thesis]: Cambridge Massachusetts Institute of Technology, 183 p
- Spencer, J.E., 1990a, Late Cenozoic extensional and compressional tectonism in the southern and western Avawatz Mountains, southeastern California: *Basin and*

- Range extensional tectonics near the latitude of Las Vegas, Nevada: Geological Society of America Memoir, v. 176, p. 317–333.
- Spencer, J.E., 1990b, Geologic map of southern Avawatz Mountains, northeastern Mojave Desert region: California: US Geological Survey Miscellaneous Field Studies Map MF-2117, scale, v. 1, no. 24, p. 000.
- Stamm, J.F., 1981, Geology at the intersection of the Death Valley and Garlock fault zones, southern Death Valley, California: Pennsylvania State University.
- Stewart, J.H., 1967, Possible large right-lateral displacement along fault and shear zones in the Death Valley-Las Vegas area, California and Nevada: Geological Society of America Bulletin, v. 78, no. 2, p. 131.
- Troxel, B.W., 1967, Sedimentary rocks of late Precambrian and Cambrian age in the southern Salt Spring Hills, southeastern Death Valley: California: California Division of Mines and Geology Special Report, v. 92, p. 33–41.
- Troxel, B.W., and Butler, P.R., 1979, Rate of Cenozoic Slip on Normal Faults, South-central Death Valley, California: Department of Geology, University of California
- Troxel, B.W., and Butler, P.R., 1998, Tertiary and Quaternary fault history of the intersection of the Garlock and Death Valley fault zones, southern Death Valley, California. In Calzia, J.E., and Reynolds, R.E., eds, Finding Faults in the Mojave: the 1998 Desert Symposium Field Guide and Volume, San Bernardino County Museum Association, p. 91-98
- Troxel, B.W., 1994, Right-lateral offset of ca. 28 km along a strand of the southern Death Valley fault zone, California: Geological Society of America Abstracts with Programs, v. 26, no. 6, p. 99.
- Unruh, J., Humphrey, J., and Barron, A., 2003, Transtensional model for the Sierra Nevada frontal fault system, eastern California: Geology, v. 31, no. 4, p. 327–330.
- Ver Planck, W. E. (1952) Gypsum in California, Calif. Div. Mines Bull. 163.
- Wright, L.A., and Troxel, B.W., 1967, Limitations on right-lateral, strike-slip displacement, Death Valley and Furnace Creek fault zones, California: Bulletin of the Geological Society of America, v. 78, no. 8, p. 933.

## APPENDICES

Appendix I. Clast count data from conglomerate beds. Q/C: quartzite or carbonate; Dio: diorite; Gr: granitic; Gn: gneiss; Vol: volcanic; Misc: unidentified

Site ID	UTM 11S	Unit	Location	Q/C	Dio	Gr	Gn	Vol	Misc
CCNH001	0549095, 3943044	nh1 (?)	DSW	5	36	53	3	0	3
CCNH002	0549177, 3943676	Tf4	DSW	12	44	20	13	4	7
CCNH003	0544983, 3949860	Tf4	Round Mnt.	20	7	21	2	50	0
CCNH004	0553510, 3940893	nh2c	CC Wash	58	25	0	13	0	4
CCNH005	0552234, 3941013	Qa2	Pipeline Wash	15	34	31	6	4	10
CCNH006	0551149, 3941234	Tf4	Behind SB	11	29	30	26	0	4
CCNH007	0551435, 3942982	nh2c	Salt Basin Papa Bear	47	19	13	19	0	2
CCNH008	0550739, 3944810	nh3	(DSW)	2	0	88	0	10	0
CCNH009	0547794, 3948052	nh3	Niter Field	0	0	92	0	8	0
CCNH010	0547725, 3947842	nh2c	Niter Field	31	17	20	26	3	3

Appendix II. Tephrochronology Lab reports. JC-NH06-T1 sample collected prior to this study (see Plate 1 for sample location).

**Sample #: JC-NH06-T1**

Listing of 37 closest matches for COMP. NO. 5465 for elements: **Na, Al, Si, K, Ca, Fe** Date of Update: 4/19/06

C.No	Sample Number	Date	SiO2	Al2O3	Fe2O3	MgO	MnO	CaO	TiO2	Na2O	K2O	Total,R	Sim. Co
<b>1</b>	<b>5465 JC-NH06-T1 T538-5</b>	<b>4/13/06</b>	<b>78.76</b>	<b>13.19</b>	<b>0.75</b>	<b>0.04</b>	<b>0.08</b>	<b>0.49</b>	<b>0.06</b>	<b>3.24</b>	<b>3.40</b>	<b>100.01</b>	<b>1.0000</b>
2	2511 91SG SJE-52A T221-1	3/8/91	78.86	12.87	0.69	0.07	0.07	0.43	0.11	3.43	3.47	100.00	0.9494
3	4969 SAM_5-012102 T490-1	10-26-02	77.66	13.13	0.77	0.04	0.09	0.49	0.06	3.82	3.95	100.01	0.9441
4	2510 91SG SJE-52A JR2/91B	2/21/91	78.79	13.23	0.71	0.08	0.04	0.44	0.13	3.54	3.03	99.99	0.9413
5	4060 M97-9 T372-10	10/97	79.36	12.85	0.72	0.07	0.05	0.43	0.11	3.40	3.02	100.01	0.9409
6	1935 NH-5 T155-8	5/15/88	77.56	13.10	0.75	0.04	0.09	0.47	0.08	4.40	3.51	100.00	0.9404
7	4949 SR-042102-1 T488-1	10-26-02	77.21	13.20	0.77	0.04	0.08	0.50	0.09	3.23	4.89	100.01	0.9376
8	4964 MOML-28M T489-6	10-26-02	78.21	12.80	0.74	0.03	0.04	0.46	0.07	3.78	3.87	100.00	0.9374
9	3518 JRK-DV-41 T325-7	7/6/95	77.18	13.23	0.75	0.04	0.07	0.48	0.07	4.60	3.57	99.99	0.9355
10	5462 HL-NH06-T2 T538-7	4/13/06	77.92	13.09	0.73	0.04	0.09	0.48	0.06	3.01	4.58	100.00	0.9343
11	3644 JRK-DV-44 T337-8	3/96	77.79	12.88	0.71	0.04	0.07	0.49	0.07	4.33	3.61	99.99	0.9335
12	1888 JT-NOVA-1 T150-6	11/9/87	77.01	13.15	0.75	0.04	0.08	0.48	0.05	3.31	5.14	100.01	0.9324
13	3520 JRK-DV-41 REV T325-7	7/6/95	77.21	13.23	0.77	0.04	0.07	0.48	0.06	4.58	3.56	100.00	0.9322
14	3948 SM-ASH 18 T359-9	3/97	79.02	12.43	0.76	0.13	0.05	0.69	0.14	3.35	3.44	100.01	0.9319
15	336 SALTON-1, T20-3		77.94	12.65	0.76	0.02	0.03	0.48	0.05	4.47	3.61	100.01	0.9303
16	1105 61384-34 ASW T82-7	10/11/84	78.09	12.58	0.73	0.08	0.05	0.51	0.10	3.70	4.17	100.01	0.9284
17	1843 FLV-19-WW T146-7	8/25/87	77.31	13.24	0.72	0.04	0.08	0.48	0.06	3.76	4.31	100.00	0.9280
18	337 SALTON-2, T2-14		77.55	12.98	0.76	0.04	0.05	0.46	0.07	4.48	3.60	99.99	0.9270
19	3497 JRK-DV-23 T323-6	5/6/95	77.38	13.18	0.71	0.04	0.08	0.48	0.07	3.73	4.33	100.00	0.9270
20	3517 JRK-DV-40 T325-6	7/6/95	77.07	13.19	0.76	0.04	0.09	0.48	0.06	4.54	3.77	100.00	0.9267
21	2319 NAP-1L T193-2	6/1/89	78.32	12.39	0.73	0.10	0.05	0.53	0.09	3.20	4.59	100.00	0.9267
22	277 PICO-43, T36-3		76.85	12.90	0.73	0.03	0.03	0.47	0.05	3.93	4.02	99.01	0.9261
23	4951 SR-042102-3 T488-3	10-26-02	77.21	13.24	0.86	0.05	0.07	0.49	0.07	3.32	4.70	100.01	0.9247
24	254 P-100, T22-4		77.78	12.86	0.75	0.03	0.05	0.45	0.06	4.27	3.75	100.00	0.9244
25	4968 AJ-02-MSE-FP T489-10	10-26-02	77.81	12.87	0.78	0.03	0.04	0.46	0.06	3.65	4.29	99.99	0.9240
26	3743 FLV-SP-8C MINOR T347-3	11/96	76.89	13.12	0.73	0.04	0.08	0.49	0.06	3.16	5.45	100.02	0.9239
27	3815 JRK-DV-SIX SP T352-5	12/96	76.99	12.83	0.74	0.04	0.07	0.49	0.06	3.28	5.50	100.00	0.9238
28	272 PICO-24, T2-16		77.34	12.89	0.76	0.04	0.03	0.49	0.07	3.84	4.53	99.99	0.9234
29	1839 FLV-16-WW T146-4	8/25/87	77.22	12.84	0.75	0.07	0.05	0.49	0.10	3.09	5.39	100.00	0.9231
30	5395 WMFZ05-09-JL T529-8	8/9/05	78.17	12.94	0.72	0.04	0.06	0.56	0.06	3.08	4.37	100.00	0.9229
31	5042 JRK-DV-219B T496-6	3-17-03	76.78	13.16	0.74	0.04	0.08	0.48	0.07	3.17	5.49	100.01	0.9228
32	4954 SR-042102-6 T488-6	10-26-02	77.62	12.93	0.80	0.04	0.06	0.47	0.08	3.59	4.42	100.01	0.9224
33	5393 WMFZ05-06A-JL T529-6	8/9/05	78.08	12.85	0.72	0.03	0.07	0.44	0.06	3.15	4.61	100.01	0.9222
34	1441 03068506A SILICIC FR. T114-1	12/12/85	77.71	12.67	0.74	0.04	0.08	0.49	0.07	3.04	5.15	99.99	0.9221
35	5276 GPS-018-04 T515-5	8-24-04	77.04	13.02	0.73	0.04	0.09	0.48	0.08	3.43	5.08	99.99	0.9220
36	4033 AF-9-2 T369-7	9/97	77.83	12.80	0.72	0.03	0.05	0.47	0.05	3.79	4.27	100.01	0.9215
37	3102 DLS-413M T289-4	11/4/93	77.02	12.99	0.75	0.04	0.08	0.47	0.05	3.18	5.44	100.02	0.9214

## SAMPLE # JN-NH-121102 T590-2

Generic similarity to DN-98 - \_\_ middle to latest Pliocene and Early Pleistocene tephra collected by D. Dethier (Williams College, Mass.) from Puye Formation, New Mexico but magnesium levels are completely off. Most closely matches 85-C768G BULK, and JY-92-46 POP-2, primary and reworked (resp.) rhyodacitic pre-Mazama (500-400 ka) tephra from Crater Lake, Oregon, and Mohawk Valley, northeastern CA (yellow highlight).

Listing of 37 closest matches for COMP. NO. 5959 for elements: Na, Mg, Al, Si, K, Ca, Ti, Fe Date of Update: 1/3/13

C.No	Sample Number	Date	SiO2	Al2O3	Fe2O3	MgO	MnO	CaO	TiO2	Na2O	K2O	Total	R	Sim. Co
1	5959 JN-NH-121102 T590-2	5/17/12	73.82	14.73	1.71	0.30	0.04	1.64	0.34	3.69	3.73	100.00	1.0000	
2	4526 DN-98-43A T420-8	11-5-99	74.15	14.44	1.61	0.35	0.03	1.41	0.34	3.78	3.88	99.99	0.9465	
3	4525 DN-98-37 T420-7	11-5-99	73.42	14.90	1.67	0.30	0.04	1.64	0.31	3.82	3.81	100.01	0.9458	
4	3043 JY-92-46 POP-2 T282-4	7/7/93	73.57	14.23	1.88	0.28	0.01	1.58	0.31	3.77	4.36	99.99	0.9594	
5	4524 DN-98-35 T420-6	11-5-99	74.14	14.41	1.54	0.35	0.04	1.46	0.34	3.60	4.11	99.99	0.9381	
6	5937 EW-062811-HL6.30 T589-1(pop2)	1/25/12	73.44	14.37	2.13	0.30	0.04	1.45	0.36	3.72	4.19	100.00	0.9355	
7	5000 PLW8/11/01P2ASH POP1 T487-3	10/26/02	75.23	13.81	1.63	0.29	0.02	1.38	0.30	3.82	3.54	100.02	0.9347	
8	4530 DN-98-100 T421-2	11-5-99	72.99	15.03	1.73	0.44	0.08	1.77	0.36	3.83	3.77	100.00	0.9329	
9	3473 ALT-22 T317-6 REDO 4/95	4/11/95	73.87	14.35	1.75	0.35	0.06	1.42	0.36	4.25	3.60	100.01	0.9314	
10	4937 PLW8/11/01_P2_ASH T487-3	10-26-02	74.95	13.89	1.67	0.35	0.02	1.43	0.31	3.87	3.51	100.00	0.9300	
11	3031 CARP-11 T281-6	6/22/93	74.49	13.78	1.93	0.32	0.03	1.39	0.37	3.99	3.70	100.00	0.9292	
12	4541 PSW-150-97-58 (silicic) T408-8 05/30/99	74.67	13.74	1.88	0.35	0.04	1.61	0.34	4.15	3.22	100.00	0.9278		
13	3861 GL2-1.55 POP1 T356-7	2/97	75.10	13.85	1.69	0.35	0.03	1.59	0.31	3.99	3.10	100.01	0.9257	
14	1734 ASW 61285-29 T-136-3	4/22/87	73.88	14.02	1.92	0.32	0.04	1.38	0.32	4.02	4.11	100.01	0.9234	
15	4533 DN-98-132 T421-5	11-5-99	73.34	14.45	1.78	0.40	0.06	1.73	0.39	3.66	4.19	100.00	0.9234	
16	2874 M91NY-41 T265-2	08/20/92	74.45	14.33	1.88	0.39	0.05	1.43	0.34	3.24	3.89	100.00	0.9190	
17	4038 PLW6997-5 POP1 T370-7	9/97	75.02	13.89	1.69	0.25	0.04	1.23	0.32	3.58	3.98	100.00	0.9184	
18	4527 DN98-65 T420-9	11-5-99	72.87											
15	05	1.80	0.45	0.07	1.87	0.33	3.94	3.63						
100	01	0.9175												
19	1753 85C768G BULK	5/29/87	73.58	14.51	1.72	0.33	0.04	1.66	0.35	5.01	2.81	100.01	0.9168	
20	4470 93RW96 T414-5	8-28-99	75.15	13.62	1.54	0.28	0.04	1.34	0.29	3.75	3.99	100.00	0.9162	
21	5390 PC-82704 T529-4	8/9/05	75.96	13.31	1.86	0.28	0.05	1.47	0.30	3.13	3.62	99.98	0.9157	
22	1368 WC-3 T104-9	8/26/85	75.25	13.95	1.64	0.28	0.05	1.14	0.31	3.87	3.51	100.00	0.9152	
23	4921 PLW8/11/01P4 T483-7	10-26-02	75.27	13.54	1.66	0.27	0.04	1.28	0.28	3.79	3.87	100.00	0.9140	
24	4523 DN-98-31A T420-5	11-5-99	73.06	14.69	1.87	0.45	0.04	1.85	0.37	3.74	3.93	100.00	0.9137	
25	3867 GL2-3.30 HI CA FE T356-9	2/97	75.29	13.75	1.70	0.39	0.02	1.67	0.31	3.91	2.96	100.00	0.9136	
26	1907 FLV-14-WW T146-2	8/25/87	74.64	13.91	1.76	0.33	0.06	1.28	0.32	4.30	3.40	100.00	0.9132	
27	1091 61284-17 ASW T81-10	9/4/84	74.79	13.44	1.90	0.32	0.05	1.40	0.29	3.60	4.21	100.00	0.9131	
28	4608 DWR-FP-9-1 T439-2	5-5-00	75.41	13.58	1.65	0.31	0.03	1.61	0.27	4.14	3.00	100.00	0.9131	
29	1306 ASW 61585 52E less sil. fr. T1	7/2/85	74.41	13.74	1.95	0.29	0.05	1.33	0.29	3.76	4.19	100.01	0.9130	
30	1381 ASW-61285-30A T108-9	9/24/85	73.82	14.03	1.96	0.30	0.03	1.31	0.30	4.06	4.20	100.01	0.9129	
31	5246 SL-02-05(416.7-417) T511-5	6-12-04	74.16	14.44	1.68	0.30	0.04	1.29	0.34	4.82	2.93	100.00	0.9120	
32	3712 CARP-13 T343-1	11/96	74.74	13.50	1.88	0.39	0.03	1.42	0.38	3.81	3.84	99.99	0.9104	
33	1071 61284-16-ASW OBSIDIAN T77-2	7/30/84	73.48	14.03	2.06	0.33	0.04	1.58	0.33	4.17	4.19	100.01	0.9093	
34	2135 FL86C-5.41 A 1 sh	73.45	14.02	2.11	0.35	0.07	1.40	0.34	4.13	4.11	99.98	0.9086		
35	3812 EL-49-RM T352-3	12/96	73.68	14.02	1.85	0.35	0.06	1.30	0.33	4.38	4.03	100.00	0.9078	
36	1054 61284-4 ASW T79-5	7/27/84	74.38	13.74	1.84	0.27	0.04	1.29	0.30	3.78	4.37	100.01	0.9067	
37	1797 61284-4 ASW (-100+200) T79-5	7/27/84	74.38	13.74	1.84	0.27	0.04	1.29	0.30	3.78	4.37	100.01	0.9067	

Listing of 37 closest matches for COMP. NO. 5959 for elements: Mg, Al, Si, Ca, Ti, Fe Date of Update: 1/3/13

C.No	Sample Number	Date	SiO2	Al2O3	Fe2O3	MgO	MnO	CaO	TiO2	Na2O	K2O	Total	R Sim.	Co
1	5959 JN-NH-121102 T590-2	5/17/12	73.82	14.73	1.71	0.30	0.04	1.64	0.34	3.69	3.73	100.00	1.0000	
2	1755 SSC76SG BULK	5/29/87	73.58	14.51	1.72	0.35	0.04	1.66	0.35	5.01	2.81	100.01	0.9741	
3	5246 SL-02-05(416.7-417) T511-5	6-12-04	74.16	14.44	1.68	0.30	0.04	1.29	0.34	4.82	2.93	100.00	0.9575	
4	4889 PNF(USGS)1 T482-1	6-22-02	73.98	14.35	1.74	0.30	0.07	1.21	0.34	5.18	2.84	100.01	0.9488	
5	3043 JY-92-46 POP-2 T222-4	7/7/93	73.57	14.25	1.88	0.28	0.01	1.58	0.31	3.77	4.36	99.99	0.9468	
6	4541 PSW-150-97-58 (silicic) T408-8 05/30/99	74.67	13.74	1.88	0.35	0.04	1.61	0.34	4.15	3.22	100.00	0.9450		
7	4890 PNF(USGS)2 T482-2	6-22-02	73.91	14.34	1.81	0.30	0.04	1.25	0.35	5.13	2.88	100.01	0.9418	
8	3861 GL2-1.55 POP1 T356-7	2/97	75.10	13.85	1.69	0.35	0.03	1.59	0.31	3.99	3.10	100.01	0.9417	
9	4455 JEO_10-8-98-1(1) T410-9	6-22-99	74.82	13.78	1.73	0.30	0.03	1.49	0.28	5.01	2.57	100.01	0.9404	
10	4526 DN-98-43A T420-8	11-5-99	74.15	14.44	1.61	0.35	0.03	1.41	0.34	3.78	3.88	99.99	0.9390	
11	4010 PLC97-3 PUM SEG#@ 78CM T366-9 6/97	73.94	14.25	1.79	0.30	0.05	1.31	0.31	5.15	2.89	99.99	0.9386		
12	601 TULELAKE-6, T69-1	12/xx/83	74.11	14.16	1.87	0.30	0.06	1.24	0.34	5.00	2.94	100.02	0.9380	
13	1068 JCD-10 T76-4	7/28/84	73.41	14.70	1.79	0.34	0.09	1.45	0.31	5.07	2.82	99.98	0.9377	
14	4524 DN-98-35 T420-6	11-5-99	74.14	14.41	1.54	0.35	0.04	1.46	0.34	3.60	4.11	99.99	0.9370	
15	4525 DN-98-37 T420-7	11-5-99	73.42	14.90	1.67	0.40	0.04	1.64	0.31	3.82	3.81	100.01	0.9369	
16	502 CAT-1, T54-8	11/25/83	73.90	14.51	1.76	0.29	0.06	1.24	0.32	4.82	3.11	100.01	0.9366	
17	3473 ALT-22 T317-6 REDO 4/95	4/11/95	73.87	14.35	1.75	0.35	0.06	1.42	0.36	4.25	3.60	100.01	0.9364	
18	4608 DWR-FP-9-1 T439-2	5-5-00	75.41	13.58	1.65	0.31	0.03	1.61	0.27	4.14	3.00	100.00	0.9349	
19	1935 LL-MFFR-1 T155-7	5/15/88	73.89	14.34	1.82	0.31	0.05	1.24	0.33	5.09	2.93	100.00	0.9344	
20	3333 RC-92 (NOO)	xx/xx/94	73.20	14.64	1.92	0.32	0.06	1.30	0.34	5.21	3.01	100.00	0.9344	
21	2687 RM-RC-3 T243-3	11/13/91	74.79	14.08	1.75	0.28	0.04	1.62	0.26	4.90	2.27	99.99	0.9343	
22	5937 EW-062811-HL6.30 T589-1(pop2)	1/25/12	73.44	14.37	2.13	0.30	0.04	1.45	0.36	3.72	4.19	100.00	0.9336	
23	1941 AV50.2-TC T155-2	5/15/88	76.61	13.03	1.74	0.30	0.05	1.80	0.29	4.03	2.15	100.00	0.9325	
24	321 RD-2(1), T7-9, pd	73.19	15.22	2.03	0.33	0.06	1.45	0.34	5.08	2.29	99.99	0.9325		
25	3958 WG96-40 POP1 T360-9	4/97	74.77	13.68	1.75	0.38	0.03	1.80	0.34	4.38	2.87	100.00	0.9323	
26	2688 RM-RC-4 T243-4	11/13/91	75.15	13.85	1.73	0.26	0.04	1.62	0.28	4.79	2.28	100.00	0.9315	
27	4451 JEO_10-1-98-2(3)B T410-5	6-22-98	74.60	13.89	1.77	0.32	0.06	1.57	0.27	5.02	2.50	100.00	0.9313	
28	4819 UO-PA-133_POP1 T471-6	10-18-01	73.82	14.17	1.92	0.31	0.04	1.30	0.35	5.18	2.91	100.00	0.9307	
29	2270 T191-3 88-B-MORAN	5/10/89	74.40	14.17	1.85	0.30	0.03	1.25	0.32	4.78	2.88	99.98	0.9303	
30	2775 #4086 T252-3	3/10/92	74.44	14.02	1.71	0.29	0.05	1.39	0.28	4.90	2.91	99.99	0.9302	
31	1067 JCD-9 T76-3	7/28/84	73.39	14.69	1.84	0.34	0.08	1.42	0.31	5.14	2.78	99.99	0.9301	
32	4977 LC080102-LCC-2 T491-5	1-11-03	74.01	14.22	1.83	0.30	0.05	1.26	0.31	5.08	2.95	100.01	0.9295	
33	2791 #4086 T252-3	4/1/92	74.23	14.29	1.69	0.30	0.06	1.36	0.27	4.97	2.83	100.00	0.9294	
34	3948 SQC-3 minor T359-6	3/97	74.38	14.19	1.83	0.31	0.05	1.27	0.32	4.70	2.95	100.00	0.9289	
35	4609 JOD_3A-4 T439-3	5-5-00	74.08	14.04	2.10	0.29	0.06	1.38	0.34	4.63	3.08	100.00	0.9287	
36	3867 GL2-3.30 HI CA FE T356-9	2/97	75.29	13.75	1.70	0.39	0.02	1.67	0.31	3.91	2.96	100.00	0.9285	
37	892 CB-34	74.06	14.25	1.79	0.30	0.05	1.21	0.31	5.12	2.91	100.00	0.9282		